R. & M. No. 3698

R. & M. No. 3698

MINISTRY OF DEFENCE (PROCUREMENT EXECUTIVE)

AERONAUTICAL RESEARCH COUNCIL
REPORTS AND MEMORANDA

The Effects of Ridge Excrescences and Trailing-Edge Control Gaps on Twodimensional Aerofoil Characteristics

By T. A. Cook

Aerodynamics Dept., R.A.E., Farnborough

LONDON: HER MAJESTY'S STATIONERY OFFICE

1972

PRICE £1·55 NET

The Effects of Ridge Excrescences and Trailing-Edge Control Gaps on Twodimensional Aerofoil Characteristics

By T. A. Cook
Aerodynamics Dept., R.A.E., Farnborough

Reports and Memoranda No. 3698*
April, 1971

Summary.

Wind tunnel measurements of the effects on twodimensional section characteristics of square ridge excrescences and of some gaps typical of those found round trailing-edge controls have been made at high subsonic Mach number and at Reynolds numbers up to $15{\cdot}6 \times 10^6$, based on section chord length. The incremental drag due to a square ridge was found to be generally underestimated by applying an estimated magnification factor to flat-plate measurements. Trailing-edge control gaps affected lift and pitching moment characteristics of the aerofoil as well as drag. A tentative correlation of the measurements of drag due to spanwise gaps is suggested.

LIST OF CONTENTS

* Replaces R.A.E. Tech. Report No. 71080—A.R.C. 33 194.

1. Introduction.

In Ref. 1 Winter and Gaudet proposed a programme of wind tunnel tests to determine the drag of many of the types of excrescence frequently present on aircraft surfaces. Some preliminary results of this programme have been published in Ref. 2, and a complete analysis of the work on twodimensional excrescences immersed in a 'flat-plate' boundary layer has been made by Gaudet and Johnson[3]. The first part of the present Report is an extension of the measurements Gaudet and Johnson made using ridges of square section mounted normal to the direction of flow, aimed at investigating the effects of pressure gradients downstream of a ridge located on an aerofoil surface. As has been pointed out by Nash and Bradshaw[4] the 'flat-plate' drag of a twodimensional excrescence is altered by a magnification factor when it is present on an aerofoil, due to the downstream pressure gradient system. The purpose of the present measurements using square ridges is therefore to compare measured drag increments with values obtained from Gaudet and Johnson's measurements scaled by an estimated magnification factor. The results obtained are expected to be typical of those for all twodimensional excrescences (e.g. steps and shallow grooves, as well as ridges), since the 'flat-plate' drag of these has been shown by Gaudet and Johnson[3] to correlate in a similar fashion, and since the magnification effect depends only on the validity of the assumption that the net effect of the excrescence is sufficiently small to be equivalent to a local increase in boundary layer momentum thickness.

The second part of this Report concerns measurements of the effects of various gaps on an aerofoil, similar to the gaps found round trailing-edge controls. The results are intended primarily as a source of data. It was not considered feasible to attempt anything like a complete definitive set of measurements in the present series of tests, and so the aim was rather to augment current scanty sources of data, e.g. that included in Hoerner's collection of drag data[5], particularly by making measurements at high subsonic Mach number and high Reynolds number. Nevertheless the present results for the drag due to spanwise gaps have been reduced to a form in which they may be applied, with care, to a rather wider variety of configurations and conditions than those included here. The effects of gaps on lift and pitching moment are also presented but are not analysed.

The sections used for this work are designated RAE 2814 and RAE 2815. Both are of recent design, and at their design conditions have a sonic 'rooftop' type of upper surface pressure distribution. In the case of Section 2814, the rooftop extends to 50 per cent chord at a Mach number of 0·72 and lift coefficient of 0·42 (at a Reynolds number of 15×10^6); this section is also designed to have a high rear loading. The rooftop on Section 2815 extends to 30 per cent chord at a Mach number of 0·66 and lift coefficient of 0·51 (at a Reynolds number of 15×10^6). The latter section was used for all the gap configurations; ridges were tested on both sections. Further information on these sections is given and experimental work on boundary layers and wakes is reported in Ref. 6.

The measurements described here were made between October, 1966, and October, 1969.

2. Experimental Details.

The measurements were made in the 8 ft × 8 ft wind tunnel at RAE, Bedford. Each of the models had a chord length of 0·76 m (30 inches), which permitted a maximum test Reynolds number of about 15×10^6 at Mach numbers up to 0·76.

The method of mounting each model in the wind tunnel is illustrated in Figs. 1 and 2. The main model supports were twin vertical struts 1·1 m apart, with additional support and the incidence control system at the tunnel side-walls. The models were mounted in an inverted position in the tunnel to maintain tension loads in the struts over the incidence range of the tests. Each model was constructed in seven spanwise panels, all of very nearly equal span and each of which was mounted on the internal support spar through a three-component balance. All the balances were of the same design, though only the three centre panels (situated between the vertical struts) had 'live', strain-gauged balances. Only the balance in the centre panel was used to provide the data presented here, the panel balances on either side of it being used solely for monitoring. Small gaps between panels prevented interference between balances; the gap on either side of the centre panel was 0·13 mm.

Each model was pressure-plotted at a section near mid-span. Pressure measurements were made using self-balancing capsule manometers; the ratio of measured pressure to tunnel stagnation pressure

was estimated to be accurate to within $\pm 0{\cdot}0003$. (Only a few of the pressure distributions measured are shown in this report; others are stored at RAE, Bedford.)

The ridges and gaps of interest here were added to each of the centre three wing panels, but not to the outboard panels. The ridges used were 1 mm square* and were glued on to the wing at the appropriate station; the configurations tested are shown in Fig. 3. The gap configurations were produced by removing the trailing edge from Section 2815 aft of 75 per cent chord, dividing the part removed from each panel into three spanwise subdivisions, and remounting each subdivision on the wing with a tie-bar (see Fig. 4). Room was left between 75 and 81 per cent chord for interchangeable blocks which either represented the spanwise gap configurations shown in Fig. 5 or restored the original wing profile. The longitudinal gap configurations shown in Fig. 6 were obtained by means of interchangeable plates fitted between the trailing edge subdivisions. Spanwise and chordwise gap configurations were not tested in combination. Some spanwise gap configurations were tested with one side of the gap sealed and faired to the initial profile; in these cases the groove in the other surface penetrated the major part of the wing thickness so that the depth to width ratio was at least 7. No 'single-sided' chordwise gap configurations were tested.

The position of boundary-layer transition on each wing surface was fixed for all tests using roughness bands which consisted of ballotini particles attached to the wing by means of thin films of adhesive. The particles used had diameters between 0·104 and 0·125 mm (0·0041 and 0·0049 inch) and the band width in all instances was 0·7 per cent chord. On the upper surface of each model the leading edge of the band was located at 4 per cent chord, and on the lower surface at 6 per cent chord. All the ridges and gaps were thus located in fully-turbulent flow, (as were the excrescences used in the work of Ref. 3).

Details of the conditions under which each configuration was tested are given in Table 1. At each condition a range of incidence was covered to give a range of C_L up to approximately 0·6 (balance load limitations restricted this range in some instances). Incidence was measured to within an estimated accuracy of $\pm 0{\cdot}02$ degrees using a strain-gauged, dead-weight device installed in the centre wing panel. Mach numbers quoted have been corrected for wind-tunnel wall blockage, and pitching moment and incidence for wall constraint effects. Drag results have been corrected for longitudinal buoyancy due to wall interference.

Possible errors in force coefficients measured at $R = 15 \times 10^6$ have been estimated to be as follows:

$$C_L : \pm 0{\cdot}001$$

$$C_m : \pm 0{\cdot}0001$$

$$C_D : \text{from } \pm 0{\cdot}0001 \text{ at } C_L = 0$$

$$\text{to } \pm 0{\cdot}0003 \text{ at } C_L = 0{\cdot}6 .$$

Errors at lower Reynolds numbers will be in inverse proportion to Reynolds number.

3. Drag Due to Square Ridge Excrescences.

Square ridge excrescences were found to have negligible effects on both the pressure distributions (other than close to the ridges) and the lift and pitching moment characteristics of the aerofoils, except when the flow in the vicinity of the ridge was supercritical (though even then effects were small); accord-

* Gaudet and Johnson[3] correlate the drag of a square ridge in terms of local surface conditions by plotting C_D/C_f against $u_\tau h/\nu$ (see Fig. 10), where u_τ is friction velocity, C_f is local skin friction coefficient, ν is kinematic viscosity evaluated at the surface, and C_D is the drag coefficient based on the frontal area of a ridge of height h and unit span. For the present work h was chosen to be large enough to give a measurable drag increment, and also so that, on the basis of estimated skin friction, $u_\tau h/\nu$ fell within the range of Gaudet and Johnson's data. The selected value of h was less than used by Gaudet and Johnson but, because the boundary layer in the present work was thinner than in their experiments, h/δ was larger, estimates being in the range 0·15 to 0·35 compared with 0·01 to 0·03.

ingly only the contribution of the ridge to drag is discussed. The increments ΔC_D were obtained by comparing smoothed drag polars with and without a ridge present; hence individual points are not shown on the experimental curves of Figs. 7, 8, 9. The drag increments amount to roughly 25 per cent of the drag of the 'clean' aerofoil in most cases, though the increment rises to nearly 50 per cent of the 'clean' aerofoil drag when the flow in the neighbourhood of the ridge is supercritical, (this is the case on Section 2815 for the ridge at 30 per cent chord at lift coefficients greater than about 0·5, and on Section 2814 at Mach numbers above 0·72 and at lift coefficients less than about 0·3).

The experimental curves of Figs. 7 to 9 are compared with two other curves, both derived from the tunnel side-wall measurements made by Gaudet and Johnson[3]. The correlations they obtained for the drag due to a square ridge are shown in Fig. 10 for Mach numbers relevant to the present work, i.e. up to 1·4. Pressure distributions measured on the present aerofoils in the absence of the ridges were used to obtain local Mach number and Reynolds number and to estimate local skin friction (*see* below for further details of this estimate), as required in the use of Gaudet and Johnson's data. The drag coefficient of Fig. 10 is based on excrescence height and local kinetic pressure, and was subsequently referred to wing chord and free stream kinetic pressure for the first of the comparisons shown in Figs. 7 to 9. The ratio of local to free stream kinetic pressures constitutes a 'first attempt' magnification factor, and the present results confirm the conclusion drawn by Nash and Bradshaw[4] that this underestimates the effect of a pressure gradient system aft of the excrescence, and that the full magnification effect can be estimated only by comparing boundary layer and wake developments with and without an excrescence present. It is however, interesting to note the insensitivity of this first estimate to lift coefficient and, for a given excrescence configuration, to Mach number. This insensitivity is due to the opposing effects of Mach number and the parameter $u_\tau h/v_w$ (primarily dependent on local skin friction) in the evaluation of C_D/C_f from Fig. 10, and to the weak dependence of C_f, when based on free stream kinetic pressure, on Mach number. An exception to this observation is the marked increase in the drag estimate shown in Fig. 9c as C_L decreases through 0·25. This is due to a sharp increase in local Mach number associated with the formation of a shock wave just downstream of the excrescence station, which is not offset by a decrease in local skin friction to the same extent as elsewhere.

Nash and Bradshaw[4] used Spence's method for calculating boundary layer momentum thickness together with the Squire and Young wake law to derive a formula for magnification factor applicable to incompressible flow. One method of extending this formula to compressible conditions would be to apply the Stewartson-Illingworth transformation to it. However it was thought worthwhile to calculate the magnification effect using a more recent calculation procedure for the compressible, turbulent boundary layer. Nash and Bradshaw's original hypothesis is retained, viz that the excrescence has only a localised effect on pressure distribution and its overall effect is simply that of a step increase in momentum thickness at the position of the excrescence, this step increase being proportional to the 'flat-plate' drag of the excrescence. The calculation of magnification factor is thus reduced to estimating the momentum thickness of the wake far downstream of the aerofoil with and without a nominal step change in momentum thickness at the position of the excrescence. The basic information used is the pressure distribution measured on the clean aerofoil.

The procedure used for estimating the momentum thickness of the far wake was available as a FORTRAN program employing the following techniques. Stagnation point was interpolated, and for each surface a laminar boundary-layer calculation was performed up to transition, essentially using the method of Rott and Crabtree[7]. Momentum thickness was assumed to be unchanged by the transition process and a starting value for the shape parameter of the turbulent boundary layer was estimated by assuming an equilibrium boundary layer and using a procedure due to Nash and Macdonald[8]. Turbulent boundary-layer development up to the trailing edge was calculated using Green's method[9]†. At the trailing edge, total momentum and displacement thicknesses were obtained by summing upper and lower surface contributions, and the momentum thickness far downstream calculated using a form of the Squire and Young wake law applicable to compressible flow[6]. A simple modification to the computer program permitted calculations to be repeated with a step increase in momentum thickness at any desired station.

† The equations used are quoted in Ref. 6.

The magnification factor so derived was found to increase slightly when the size of the step was increased, and the size of the step chosen was therefore approximately the momentum deficit corresponding to the flat-plate drag of the ridge. No step change in shape parameter was fed into the calculation since boundary layer calculations made in another context had shown that an error in shape parameter at a particular station very quickly disappeared as the calculation proceeded downstream. In some cases magnification factor could not be estimated at high C_L since boundary-layer separation was predicted (it may be noted that the effect of the step increase in momentum thickness on the value of C_L at which separation first occurred was small). Some examples of the magnification factor obtained for Section 2815 are shown in Fig. 11 and compared with experimental data (i.e. the ratio of present results to 'unmagnified' Gaudet and Johnson data) and also with values obtained using both Nash and Bradshaw's formula for incompressible flow and their formula modified by the Stewartson-Illingworth transformation*. Comparison of the estimation methods shows that taking account of compressibility reduces magnification factor and that the present method and the transformed Nash-Bradshaw formula give very similar results. For the cases shown, experimental results agree well with present estimates at low lift coefficient, but increase more rapidly with increasing lift than do the estimates.

The final comparisons of Figs. 7, 8, 9 show a general tendency for drag increments to be underestimated by the method described above. The results shown for Section 2814 at $M=0{\cdot}769$ (Figs. 8 and 9) are considered first. It must be pointed out that pressure distributions on the 'clean' aerofoil show that the ridge was located near the position of peak velocity on the lower surface and that at this Mach number the flow is locally supercritical at lift coefficients less than 0·4. At a lift coefficient about 0·25 a shock wave forms just aft of the excrescence station and as lift coefficient decreases below 0·25 the strength of the shock wave increases while its position remains virtually unchanged. In association with this shock wave development the velocity at the excrescence station increases sharply, as noted previously. The estimate of drag increment due to the ridge is evidently too small when no shock wave is present on the clean aerofoil and too large when there is a shock wave present. The latter effect is most probably due to the effect of the additional disturbance of the ridge on the position and strength of the shock wave; at higher values of C_L, when no shock wave exists on the lower surface of the clean section, it is probable that the disturbance due to the ridge is sufficiently large to create a shock wave at or aft of the excrescence. In either case the estimation method must fail since it does not account for changes in the pressure distribution due to the formation of a shock-wave nor for shock-boundary layer interactions. The flow in the vicinity of the ridge is also close to critical or just supercritical in the case of Section 2814 at $M=0{\cdot}725$ (Fig. 8), and in that of Section 2815 for the ridge at 30 per cent chord and at lift coefficients greater than about 0·4 (Fig. 7a); in these cases the measurements are probably underestimated for the same reason.

Elsewhere for Section 2815 (Fig. 7) good agreement between estimate and measurement is obtained. The measurements on Section 2814 at $M=0{\cdot}601$ and 0·661 are estimated well at a Reynolds number of $7{\cdot}5\times10^6$ (Fig. 8), but are significantly underestimated at a Reynolds number of 15×10^6 (Fig. 9). A partial explanation of this result lies in the relatively large size of excrescence used. Good and Joubert[11] suggest that the type of correlation obtained by Gaudet and Johnson is valid only when the excrescence lies within the law of the wall region of the undisturbed boundary layer, and that the drag of a twodimensional excrescence which extends beyond the log-law region will be greater than that predicted using Gaudet and Johnson's data, (the excrescences used by Gaudet and Johnson were well within the law of the wall region). Calculations based on boundary layer measurements made on the present sections[6] show that the outer limit of validity of the law of the wall is roughly $0{\cdot}1\delta$ less than the excrescence height at $R=15\times10^6$. However this difference is not expected to be very sensitive to Reynolds number, so that this argument can explain only why the present estimates should be low on average and not the apparent large Reynolds number effect shown. The change in the level of agreement in going from one Reynolds number to the other must therefore be attributed to experimental error; the differences are in fact less than the possible differences suggested by the errors quoted in Section 2. On average the estimates for all the cases not likely to be affected by shock-wave development are about 10 per cent less than measurements.

---

* Boundary-layer parameters estimated by Green's method were used in these formulae.

4. Effects of Gaps and Grooves.

In this section the term 'gap' is used to indicate a configuration where there is an unrestricted air passage from surface to surface; the term 'groove' is used where there is no air passage, i.e. one side of a gap is sealed.

All of the gap configurations were found to affect each of drag, lift and pitching moment of the aerofoil (Section 2815). Thus all three components have been plotted for each gap configuration, at a Reynolds number of 15×10^6, and these are shown in comparison with the clean configuration in Figs. 12 to 21. (Fig. 5 should be referred to for specifications of the spanwise gap configurations *A*, *B*, *C*, *D*, *E*; the chordwise gap configurations labelled *F* and *G* are detailed in Fig. 6.) In addition to the not-unexpected increase in drag due to each of the gaps, they affect other components qualitatively as follows:

(i) a reduction in the effective camber of the section, as demonstrated by a reduction in lift coefficient at zero incidence and a reduction in the absolute magnitude of pitching moment at zero lift, and in the case of spanwise gaps only,

(ii) a small decrease in lift-curve slope,

(iii) a small forward shift of aerodynamic centre.

A typical comparison of pressure distributions with and without a spanwise gap is shown in Fig. 22 for constant incidence. Here it is shown that the gap affects the pressure distribution over the entire aerofoil; the loading just upstream of the gap is reduced, the loading just downstream increased by the presence of the gap, and the overall circulation is decreased. Some comparisons of pressure distributions at constant C_L are shown in Figs. 23 and 24, from which it is evident that there is a net loss of lift aft of about 40 per cent chord which is offset by the increase upstream of 40 per cent chord induced by the additional incidence of the section with a gap present. These observations readily explain item (i) above, which is the primary effect.

Overall drag increments for all gap configurations are shown in Fig. 25 for $R = 15 \times 10^6$, the curves being differences between the mean curves drawn in Figs. 12 to 14. Corresponding increments for the groove configurations tested are shown in Fig. 26 (the grooves were found to have negligible effects on lift and pitching moment); if possible experimental errors are borne in mind, these increments are seen to be very small and very nearly constant up to $C_L \simeq 0{\cdot}4$, except for configuration *E* with the groove on the upper surface where there is a greater dependence on C_L*.

The effect of Reynolds number on the drag due to gaps is shown in Fig. 27 for zero lift and is seen to be small in comparison with expected experimental errors.

The results described show that the effects of gaps cannot be properly treated as being due to a localised disturbance of the boundary layer, as were the effects of ridges. Any complete estimation method would have to take into account changes in overall pressure distribution, and the derivation of a procedure to do this is outside the scope of the present work. However an attempt to correlate the present drag results for spanwise gaps has been made, with the intention of making the results more generally useful. It is assumed that Reynolds number effects can be neglected, which implies that drag increments are not sensitive to local boundary-layer parameters. It also seems plausible to suggest that Mach number effects will be small, provided the flow over the wing in the vicinity of the gap is subcritical. The other factors determining gap drag are likely to be the width and length of the gap, the pressure difference across the gap, and the geometry of each of the gap/wing surface junctions. The effect of gap width at $R = 15 \times 10^6$ has been examined in the two instances where this was varied, and a reasonable collapse of the results for different widths was obtained by assuming incremental drag to be proportional to $(W/c)^{3/5}$, where W is gap width and c is the section chord length. The collapse obtained is illustrated in Fig. 28. The length l of the air passage of each gap configuration was not varied, but it seems likely that the drag is dependent on the mass flow through the gap and, to a first approximation for laminar or turbulent viscous flow through a long, narrow twodimensional channel, mass flow depends on a power of the factor W^3/l. It is therefore assumed that incremental drag is proportional to $(W^3/c^2 l)^{1/5}$, and Fig. 29 shows plots of $\Delta C_D (lc^2/W^3)^{1/5}$ against $C_{p_{LS}} - C_{p_{US}}$, where $C_{p_{LS}}$ is pressure coefficient on the clean aerofoil at the position of the gap entry on the lower surface and $C_{p_{US}}$ is that on the upper surface.

---

* The result for configuration *E* is commented on later.

If possible experimental errors are borne in mind, Fig. 29 shows consistent results for configurations *A, B, C, D.* If it is assumed that the incremental drag for zero pressure difference is the combined drag of the two grooves, a mean value for this can be obtained from Fig. 26 and a general trend for the results for these configurations established. This trend is included in Fig. 29. The factor which has not so far been discussed, viz gap entry and exit geometry, may account for the different trend shown by the results for configuration *E*: it is seen in Fig. 5 that there is a sharp lip downstream of the upper surface gap for configuration *E*, whereas the corresponding lip for other configurations is rounded. It will also be recalled that the drag due to an upper surface groove of configuration *E* behaved differently from that due to other groove configurations (Fig. 26), so that it seems possible that the different results for configuration *E* are due to interference of this lip with the flow. The fact that grooves of configuration *E* show a negative drag increment at lift coefficients above 0·2 appears to be a genuine result, though it is difficult to visualise the nature of a local effect which results in a reduction in boundary-layer momentum thickness (as the results imply), particularly when the corresponding surface-to-surface gap produces quite the opposite effect. However it does seem that the correlation shown for the other configurations is only applicable to cases where the gap entries and exits are carefully designed. Without similar work on a number of aerofoils, the results of Fig. 29 should be used with caution in applying them to other types of pressure distribution.

No attempt to establish any correlation for the drag due to chordwise gaps has been made, though Fig. 25 shows that for $C_L \lesssim 0{\cdot}2$, the incremental drag for configuration *F* is double that for configuration *G*, i.e. over this range the drag increment is proportional to gap width.

5. Conclusions.

Measurements of the incremental drag due to a square ridge excrescence on a twodimensional aerofoil suggest that the estimation method outlined in Section 3 is unlikely to give meaningful results when the flow in the vicinity of the excrescence station is supercritical on the clean aerofoil, and is likely to give a large underestimate when the disturbance due to the excrescence results in the formation of a shock wave. Otherwise incremental drag is under-estimated by about 10 per cent on average and this is thought to be due, at least partly, to the fact that the excrescences used were larger than the region of validity of the law of the wall, which is likely to be the region within which the 'flat-plate' correlation used[3] is also valid. Magnification factors estimated by applying the Stewartson-Illingworth transformation to the Nash-Bradshaw formula for incompressible flow[4] are similar to those obtained herein.

Trailing-edge control gaps affect lift and pitching moment characteristics of the aerofoil as well as drag. A correlation of drag increments due to spanwise gaps has been suggested in this Report, but the main value of the measurements is likely to be their addition to other results for gap effects.

LIST OF SYMBOLS

M	Corrected free stream Mach number
R	Reynolds number, based on chord length
α	Corrected incidence (degrees)
b	Span of centre panel of model, i.e. panel on which measurements were made
c	Wing chord length
h	Ridge height
l	Surface-to-surface length of spanwise gap
W	Width of gap
X	Chordwise distance from leading edge of aerofoil
C_p	Pressure coefficient
C_L	Lift coefficient
C_m	Pitching moment coefficient, referred to leading edge
C_D	Drag coefficient
ΔC_D	Increment in drag coefficient due to excrescence or gap
δ_2	Boundary layer momentum thickness

REFERENCES

No.	*Author(s)*	*Title, etc.*
1	K. G. Winter and L. Gaudet ..	A programme of tests on the drag of excrescences proposed for the 8 ft × 8 ft wind tunnel and a brief analysis of some previous measurements. Unpublished MAS material (1967).
2	K. G. Winter and L. Gaudet ..	Some recent work on compressible turbulent boundary layers and excrescence drag. NASA SP 216 (Paper No. 15) (1968).
3	L. Gaudet and P. Johnson ..	Measurements of the drag of various twodimensional excrescences immersed in turbulent boundary layers at Mach numbers between 0·2 and 2·8. RAE Technical Report 70190, ARC 32848 (1970).
4	J. F. Nash and P. Bradshaw ..	The magnification of roughness drag by pressure gradients. *Journal R. Ae. S. Vol. 71, p. 673 (1967).*
5	S. F. Hoerner	*Fluid-dynamic drag.* Published by author, New York (1965) edition.
6	T. A. Cook	Measurements of the boundary layer and wake of two aerofoil sections at high Reynolds number and high subsonic Mach number. RAE Technical Report 71127 (1971).
7	N. Rott and L. F. Crabtree ..	Simplified laminar boundary-layer calculations for bodies of revolution and for yawed wings. *J. Aero. Sciences, Vol. 19(8), pp. 553–565 (1952).*
8	J. F. Nash and .. .. .. A. G. J. MacDonald	The calculation of momentum thickness in a turbulent boundary layer at Mach numbers up to unity. A.R.C. C.P. No. 963 (1966).
9	J. E. Green	Application of Head's entrainment method to the prediction of turbulent boundary layers and wakes in compressible flow. RAE Technical Report (to be published).
10	M. C. P. Firmin and .. .. T. A. Cook	Detailed exploration of the compressible, viscous flow over two-dimensional aerofoils at high Reynolds number. ICAS Paper 68–09, Unpublished MAS material (1968).
11	M. C. Good and P. N. Joubert	The form drag of two-dimensional bluff-plates immersed in turbulent boundary layers. *Journal of Fluid Mechanics, Vol. 31 (3), pp. 547–582 (1968).*

TABLE 1

Test Conditions.

Section	Configuration	Reynolds No.	Mach No.
2814	Ridge at 43% lower surface	$7{\cdot}5 \times 10^6$	0·601
	Ridge at 43% lower surface	$7{\cdot}5 \times 10^6$	0·661
	Ridge at 43% lower surface	$7{\cdot}5 \times 10^6$	0·725
	Ridge at 43% lower surface	$7{\cdot}5 \times 10^6$	0·769
	Ridge at 43% lower surface	15×10^6	0·601
	Ridge at 43% lower surface	15×10^6	0·661
	Ridge at 43% lower surface	15×10^6	0·769
2815	Ridge at 30% upper surface	$15{\cdot}6 \times 10^6$	0·665
2815	Ridge at 60% upper surface	$15{\cdot}6 \times 10^6$	0·665*
2815	Gap configurations *A*, *B*, *C*, *D*, *E*, *F*, *G*	15×10^6	0·665
	Gap configurations *A*, *B*, *C*, *D*, *E*, *F*, *G*	10×10^6	0·665*
	Gap configurations *A*, *B*, *C*, *D*, *E*, *F*, *G*	5×10^6	0·665*
2815	Groove configuration *A* (lower surface)	15×10^6	0·665
	Groove configuration *C* (upper surface)	15×10^6	0·665
	Groove configuration *E* (upper surface and lower surface)	15×10^6	0·665

* Reduced incidence range covered.

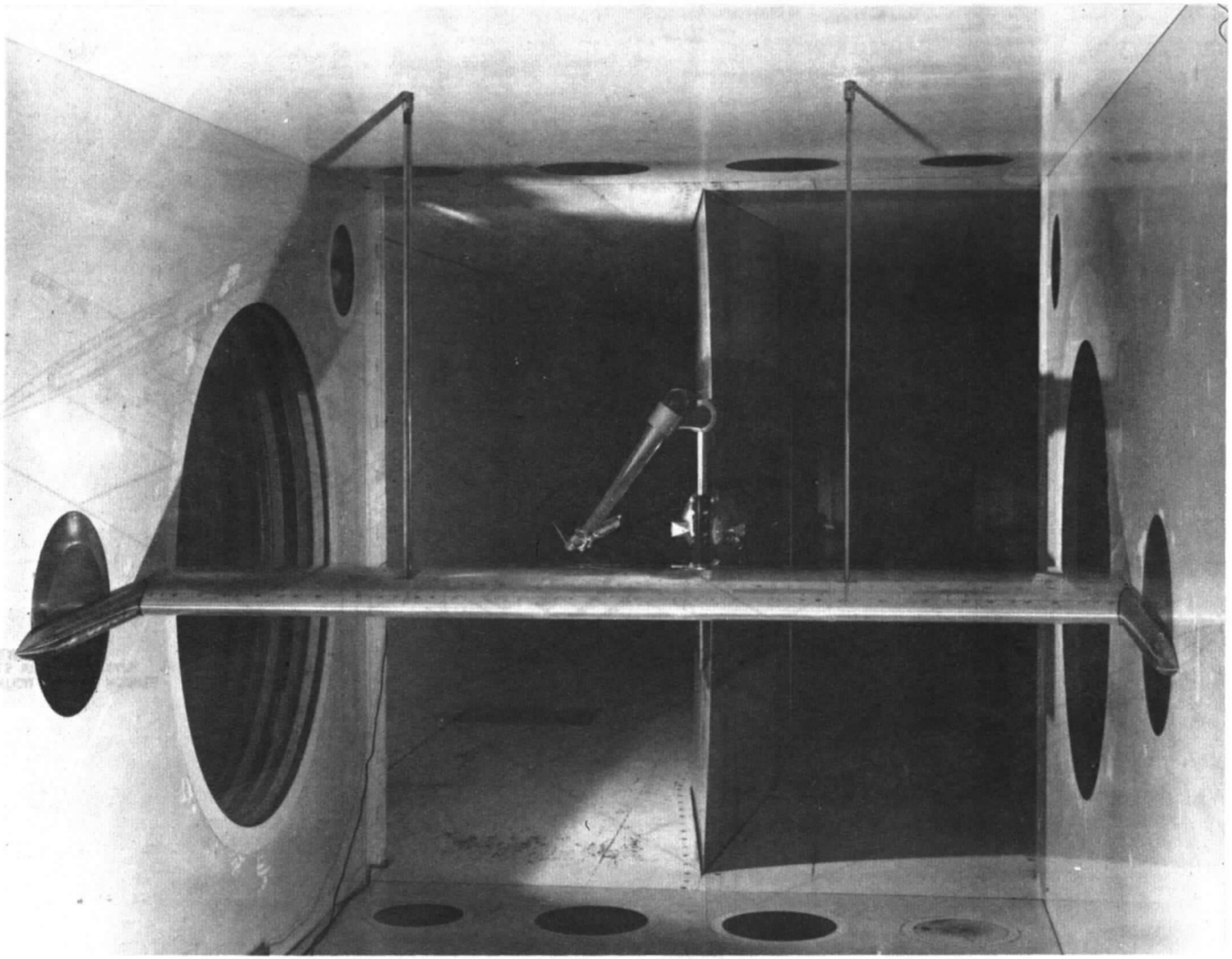

FIG. 1. The complete model.

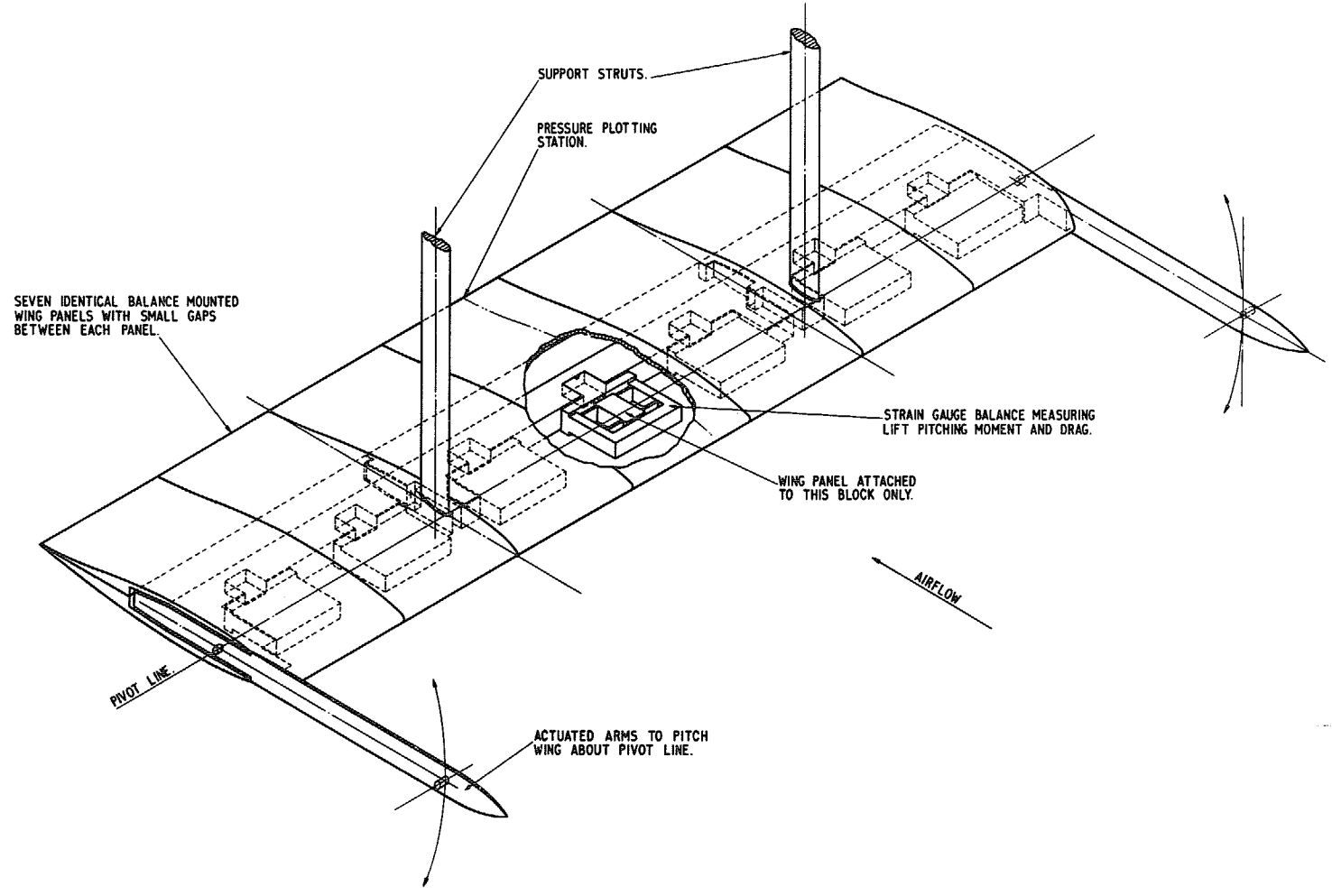

FIG. 2. Isometric view of model.

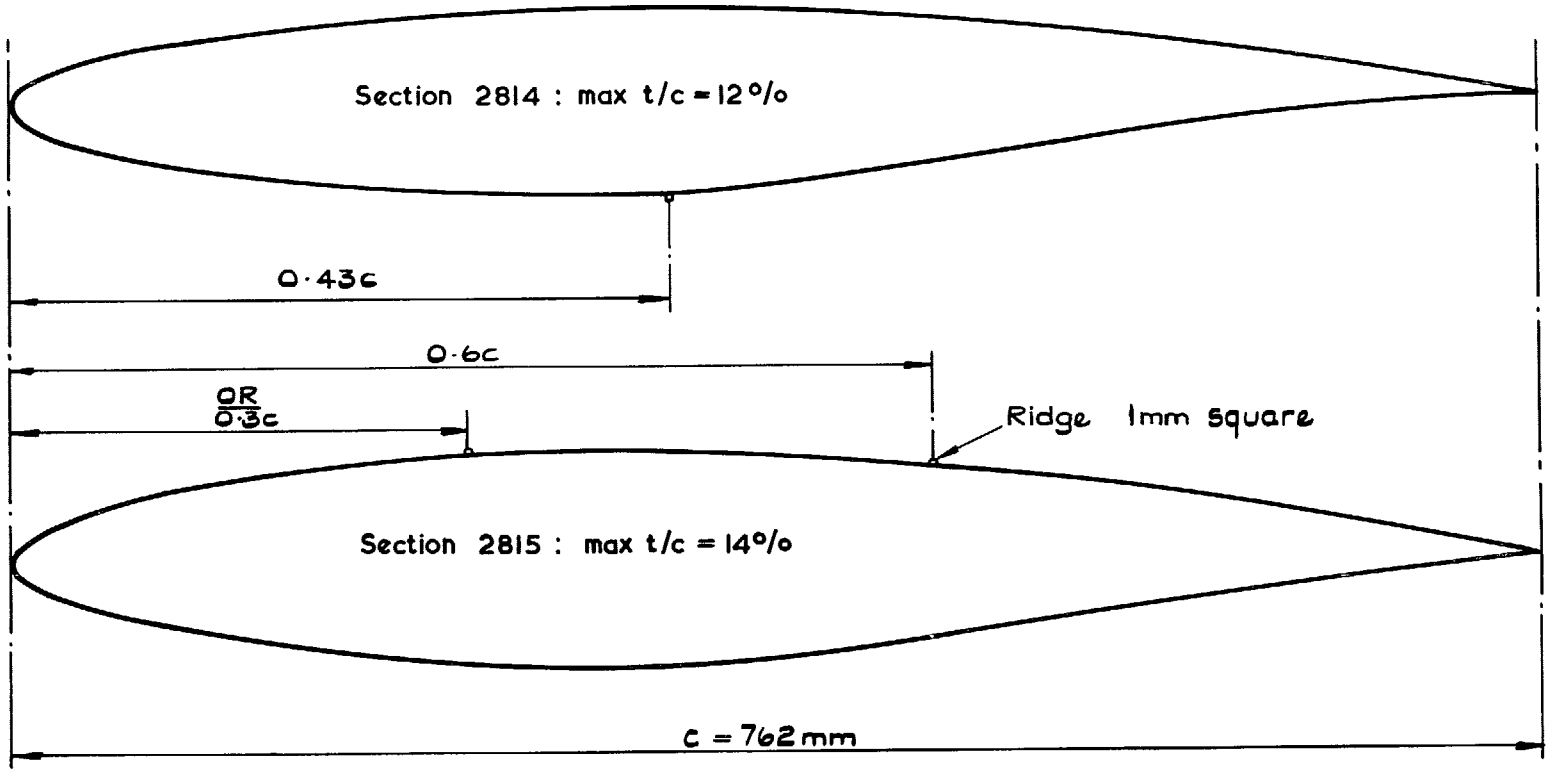

FIG. 3. Location of ridges on wing sections.

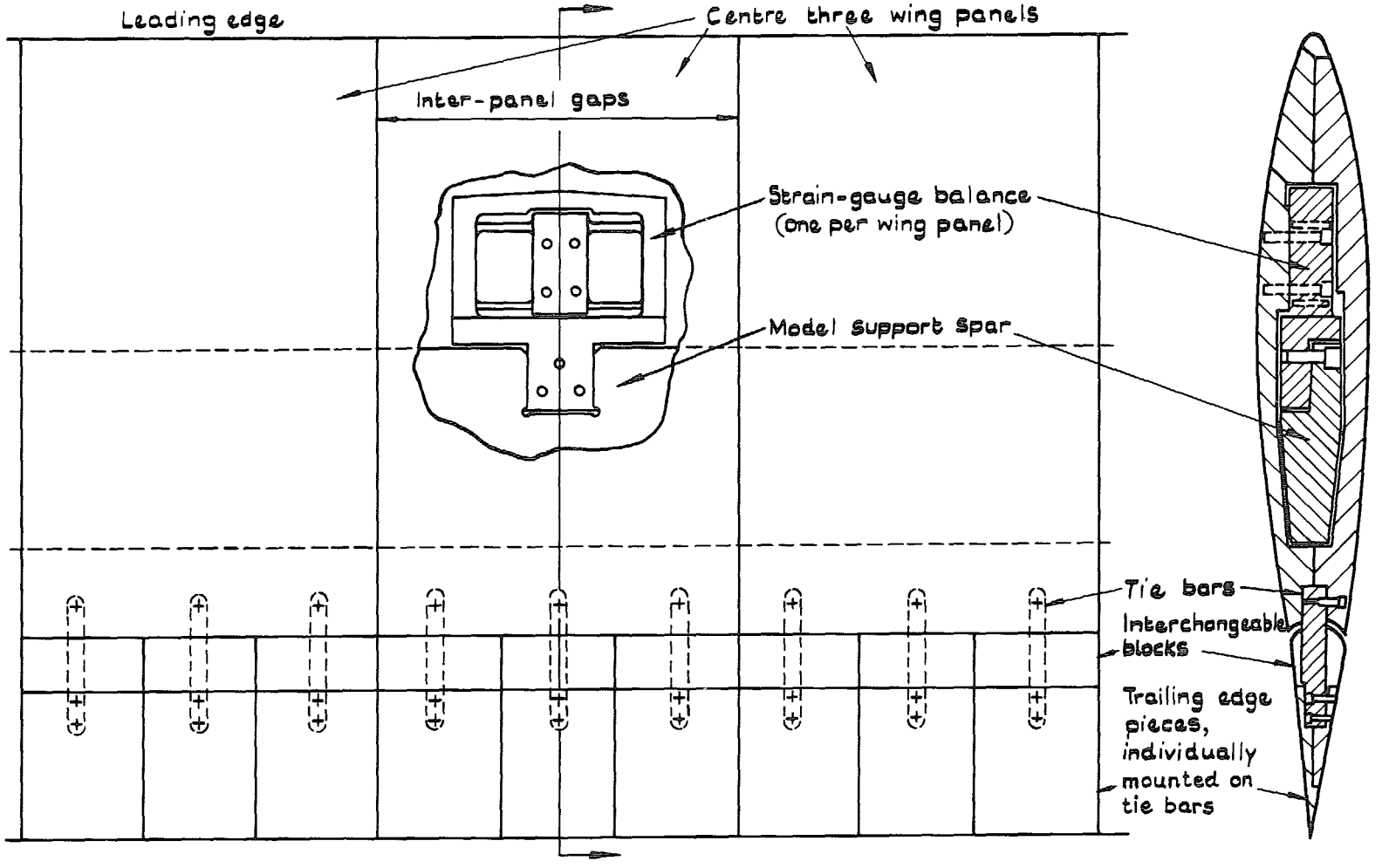

FIG. 4. Model arrangement for trailing edge gap configurations tested on Section 2815.

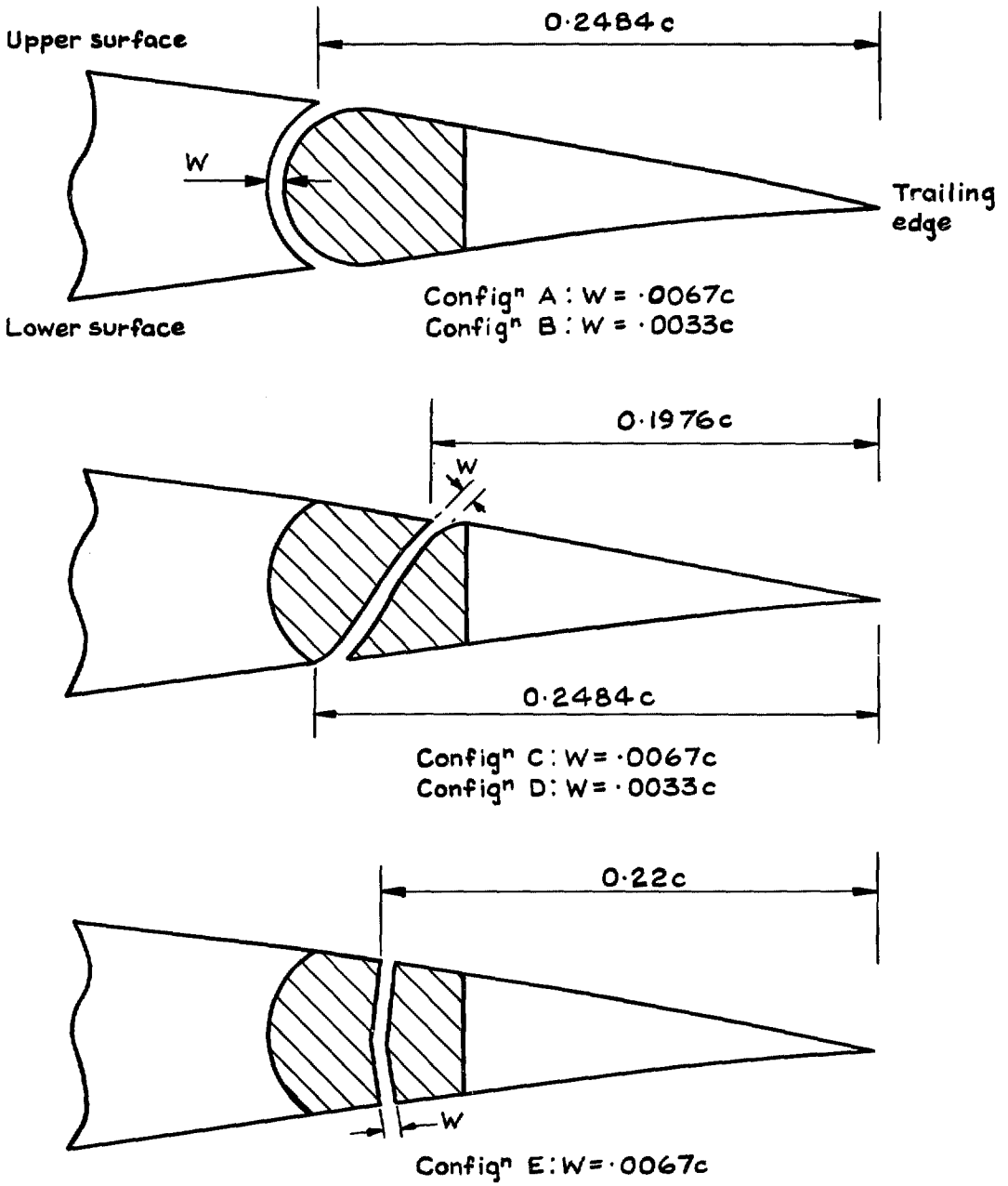

FIG. 5. Spanwise gap configurations.

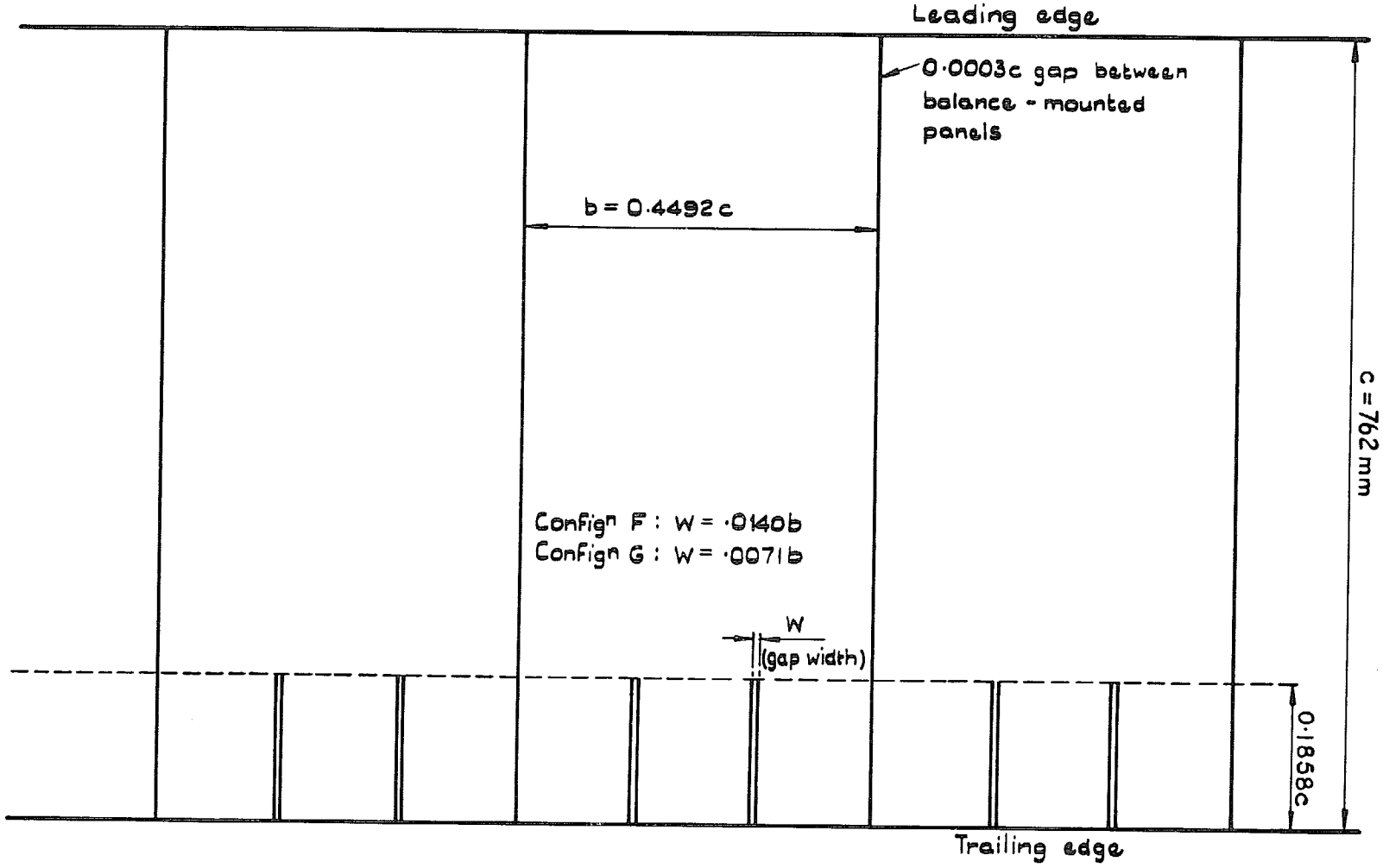

FIG. 6. Chordwise gap configurations (plan view).

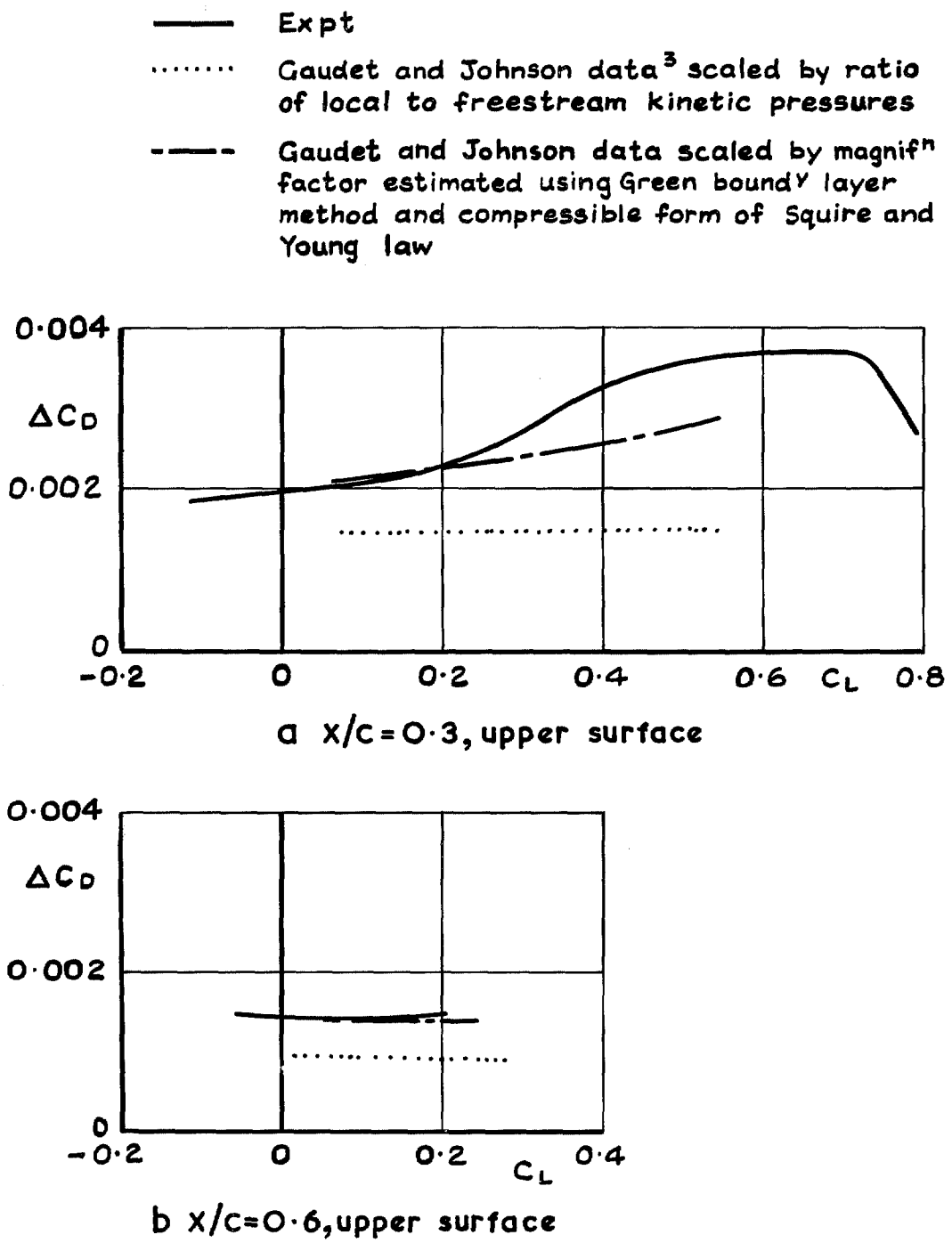

FIG. 7a & b. Drag due to square ridge excrescence: Section 2815; $M = 0{\cdot}665$, $R = 15{\cdot}6 \times 10^6$.

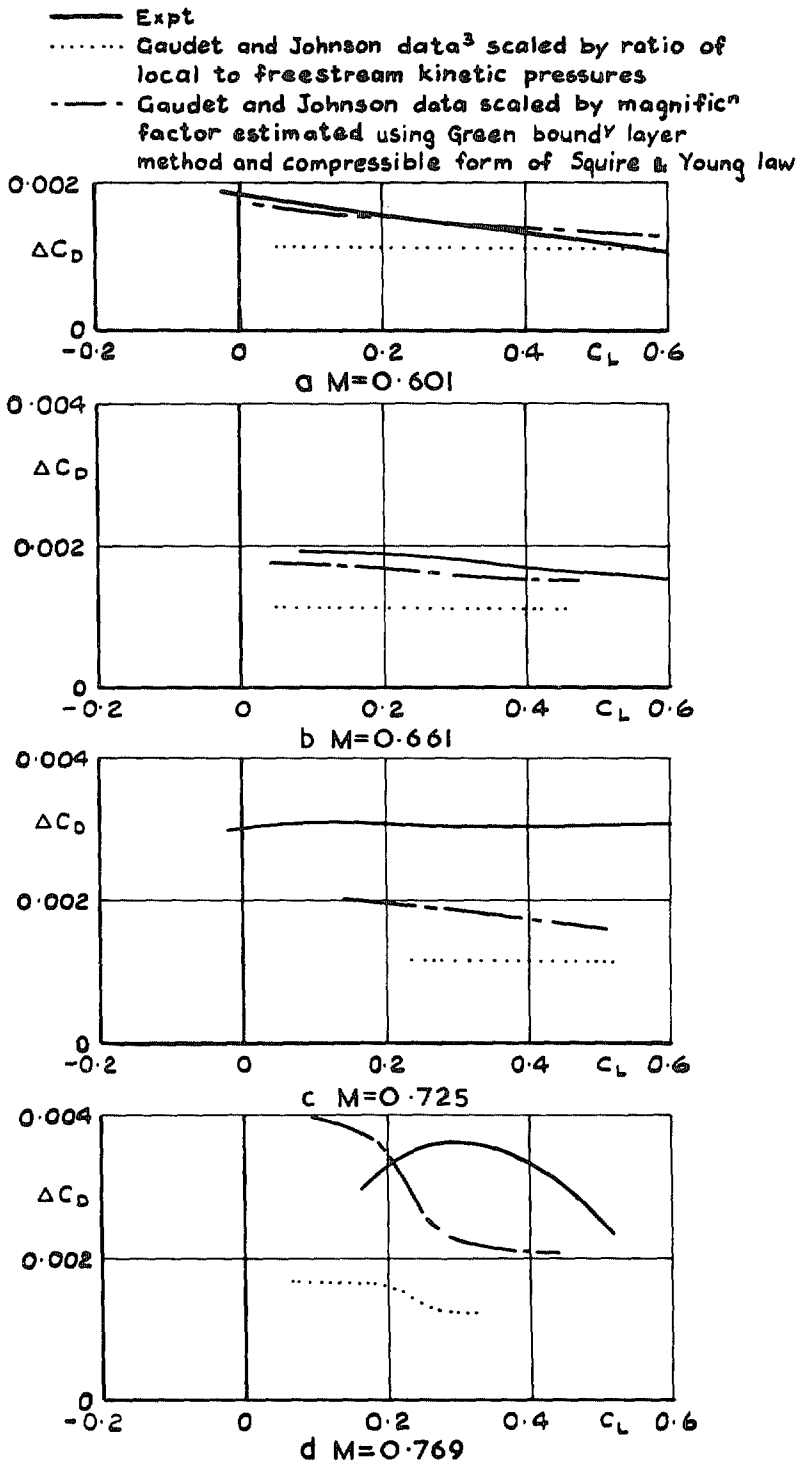

FIG. 8a–d. Drag due to square ridge excrescence at $x/c = 0{\cdot}43$ on lower surface of Section 2814: $R = 7{\cdot}5 \times 10^6$.

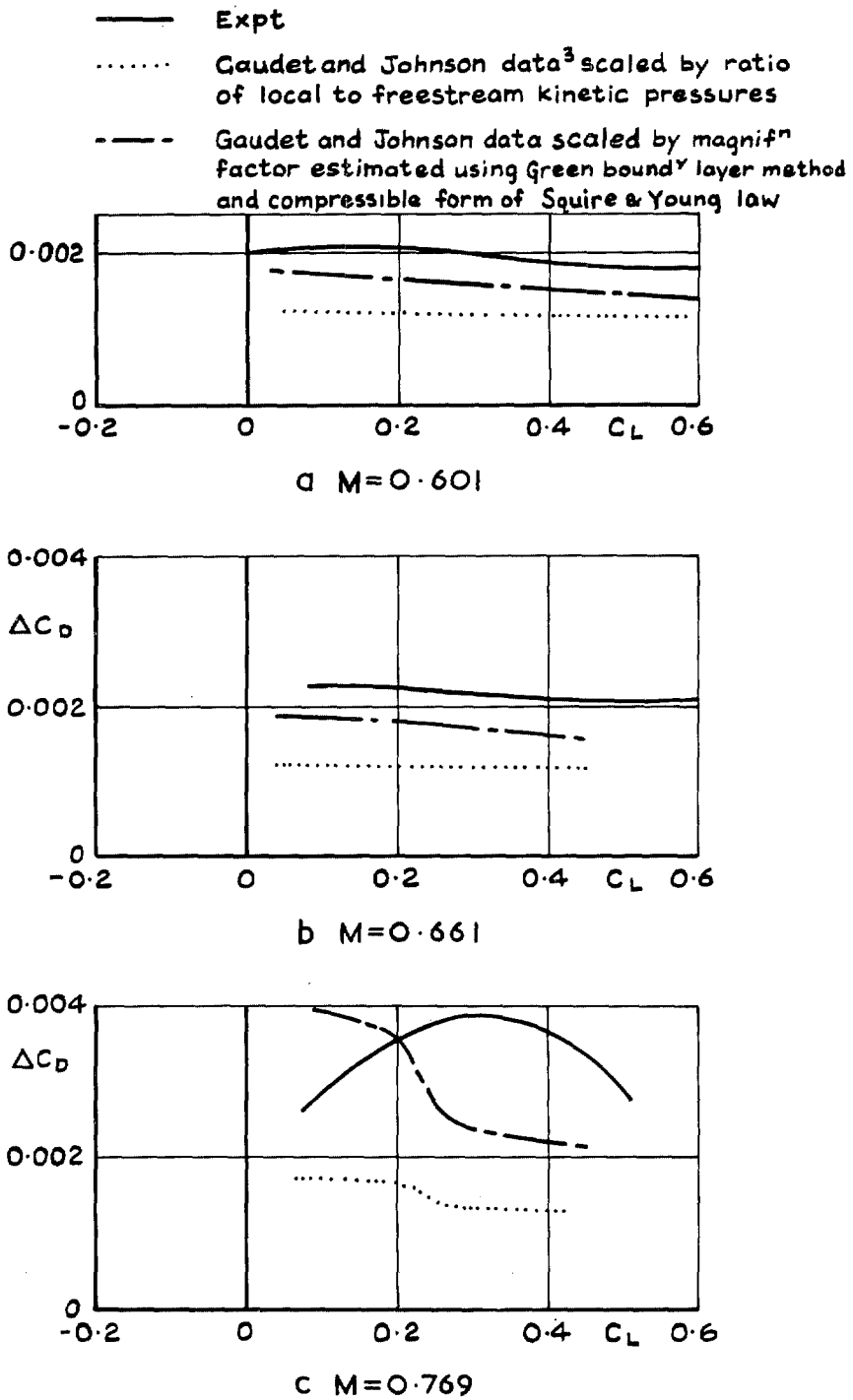

FIG. 9a–c. Drag due to square ridge excrescence at $x/c = 0{\cdot}43$ on lower surface of Section 2814: $R = 15 \times 10^6$.

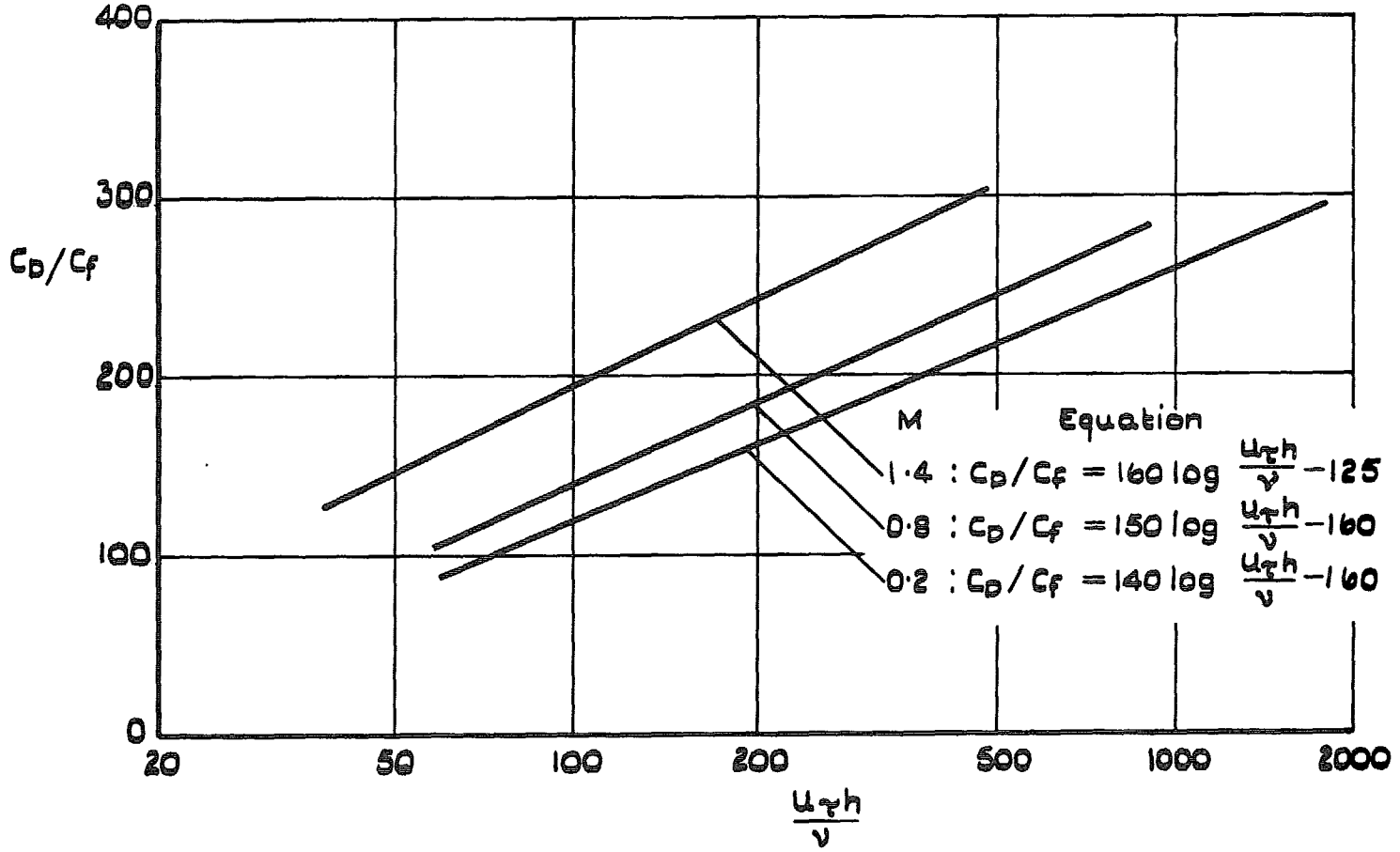

FIG. 10. Correlation curves for drag of square ridge on tunnel side-wall (from Gaudet and Johnson: Ref. 3).

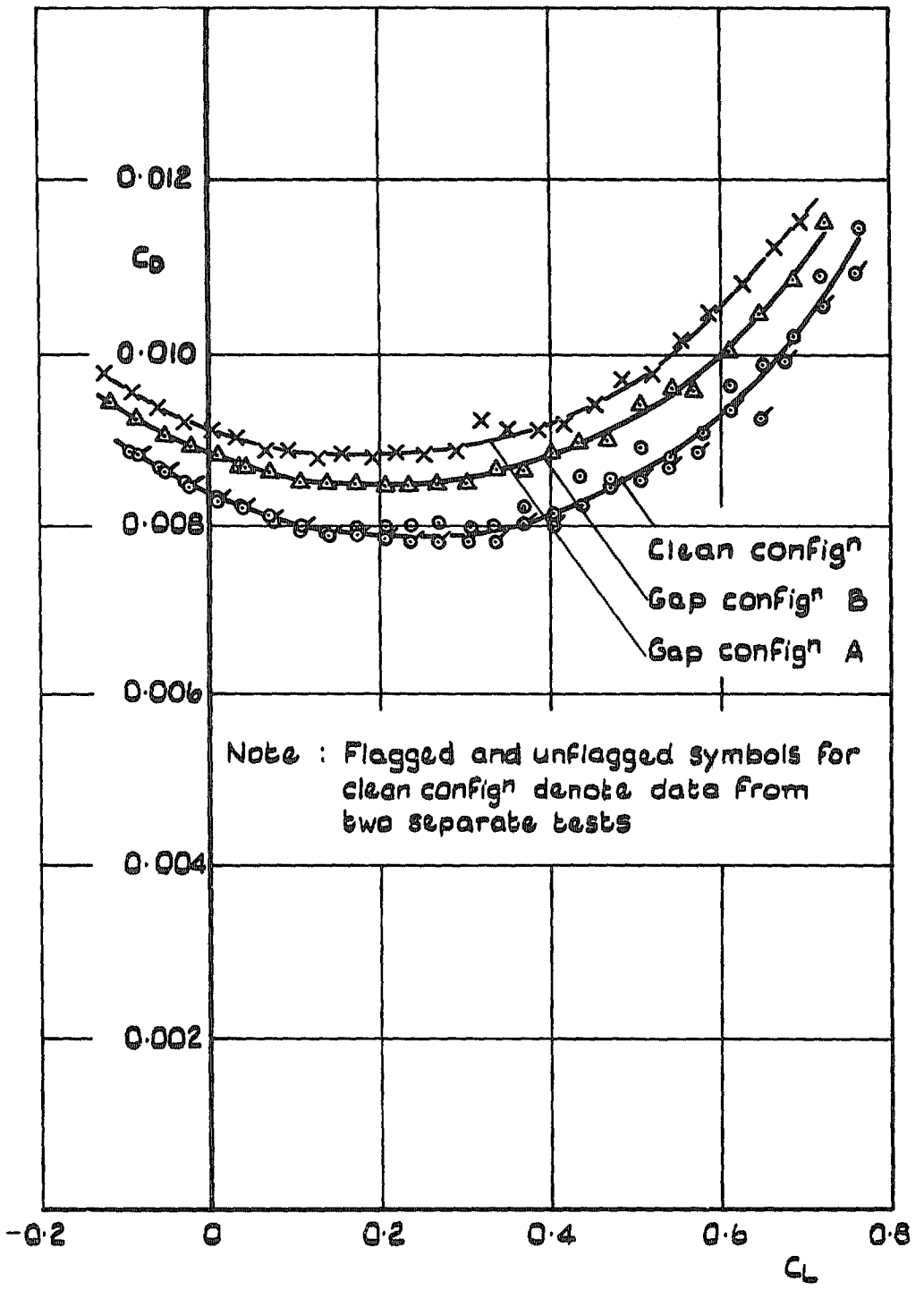

FIG. 12. Drag polars for spanwise gap configns A and B: $R = 15 \times 10^6$.

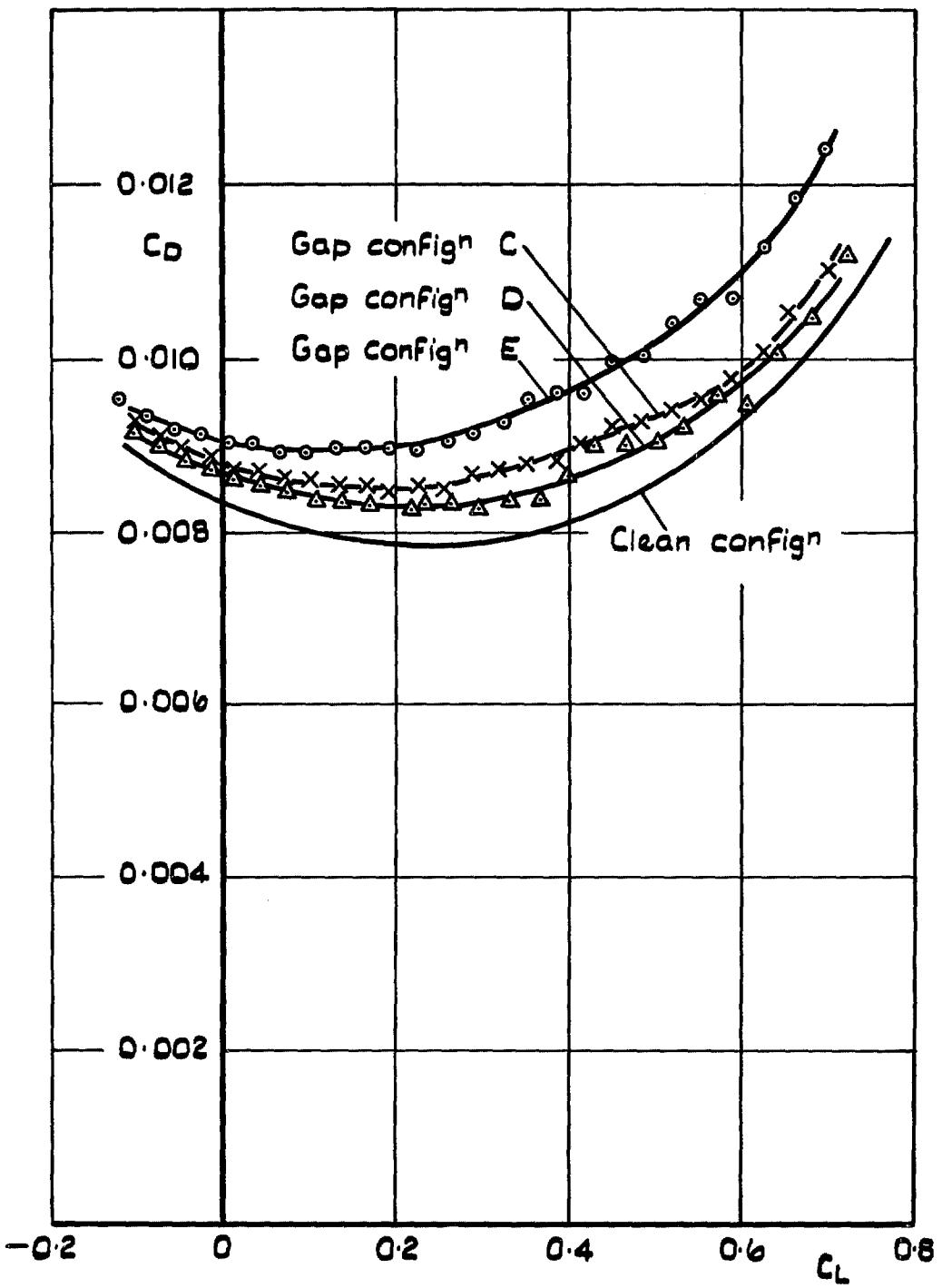

FIG. 13. Drag polars for spanwise gap configns C, D, E: $R = 15 \times 10^6$.

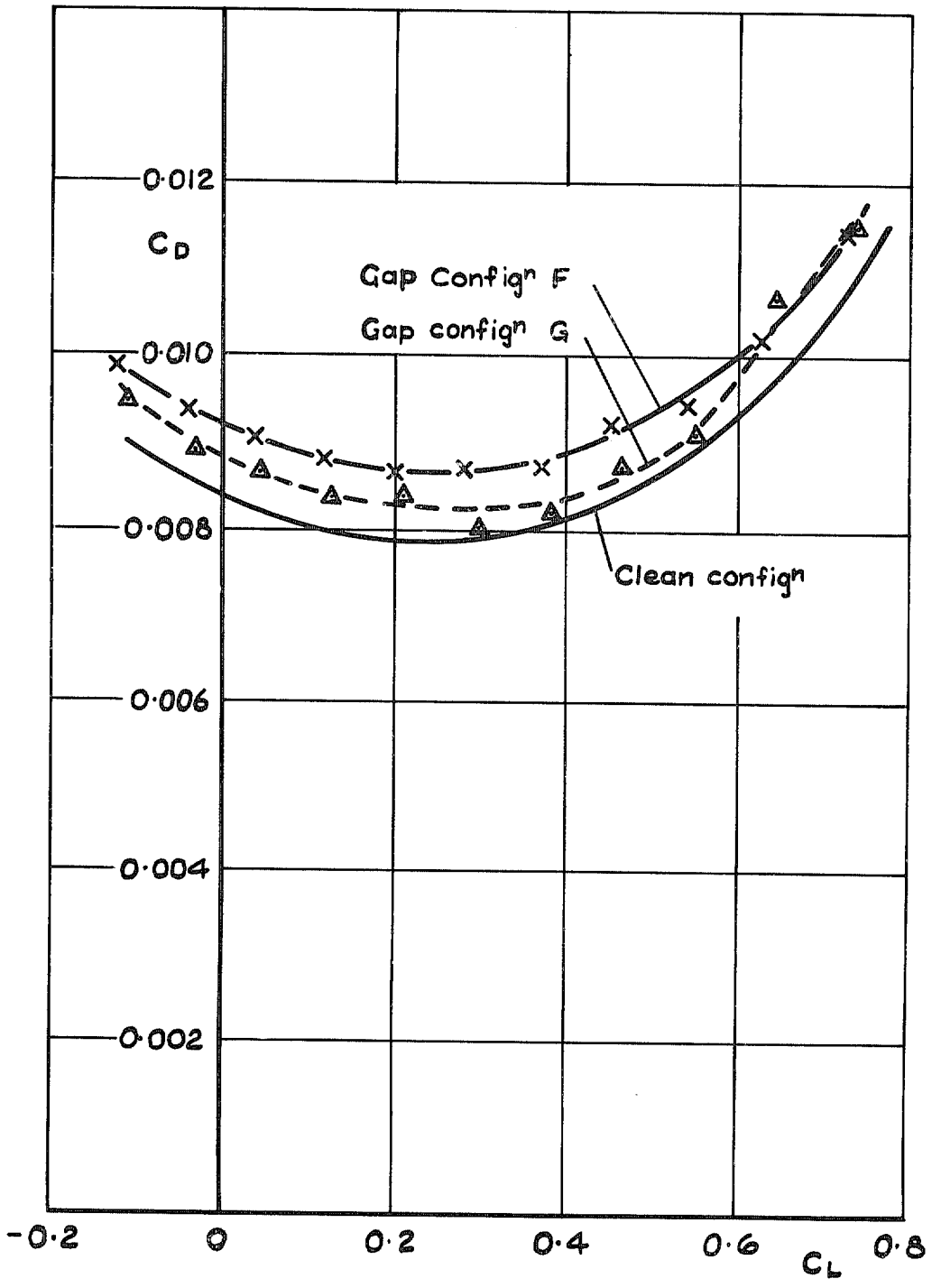

FIG. 14. Drag polars for chordwise gap configns F and G: $R = 15 \times 10^6$.

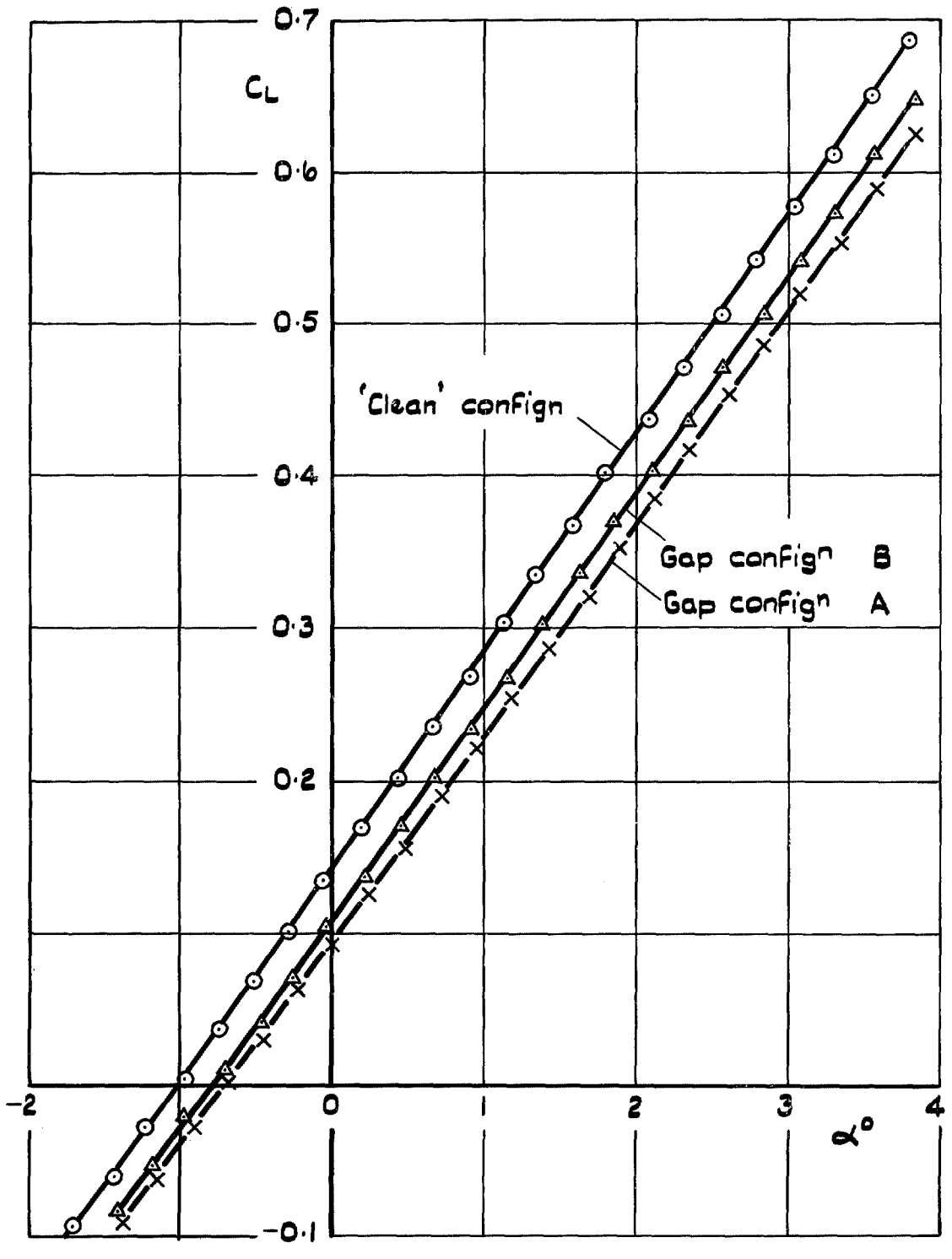

FIG. 15. Effect of spanwise gaps on C_L v α configns A and B: $R = 15 \times 10^6$.

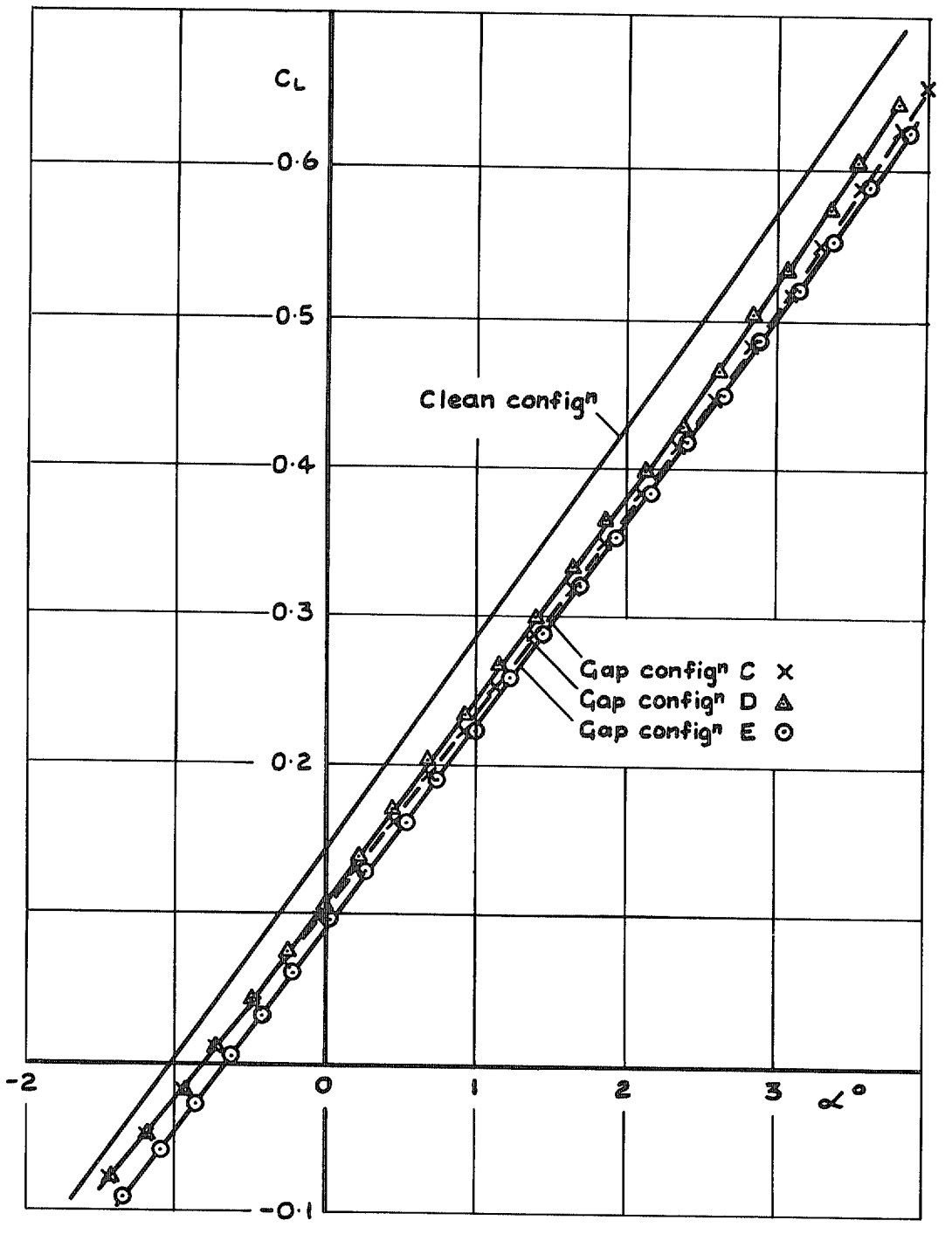

FIG. 16. Effect of spanwise gaps on C_L v α configns C, D, E: $R = 15 \times 10^6$.

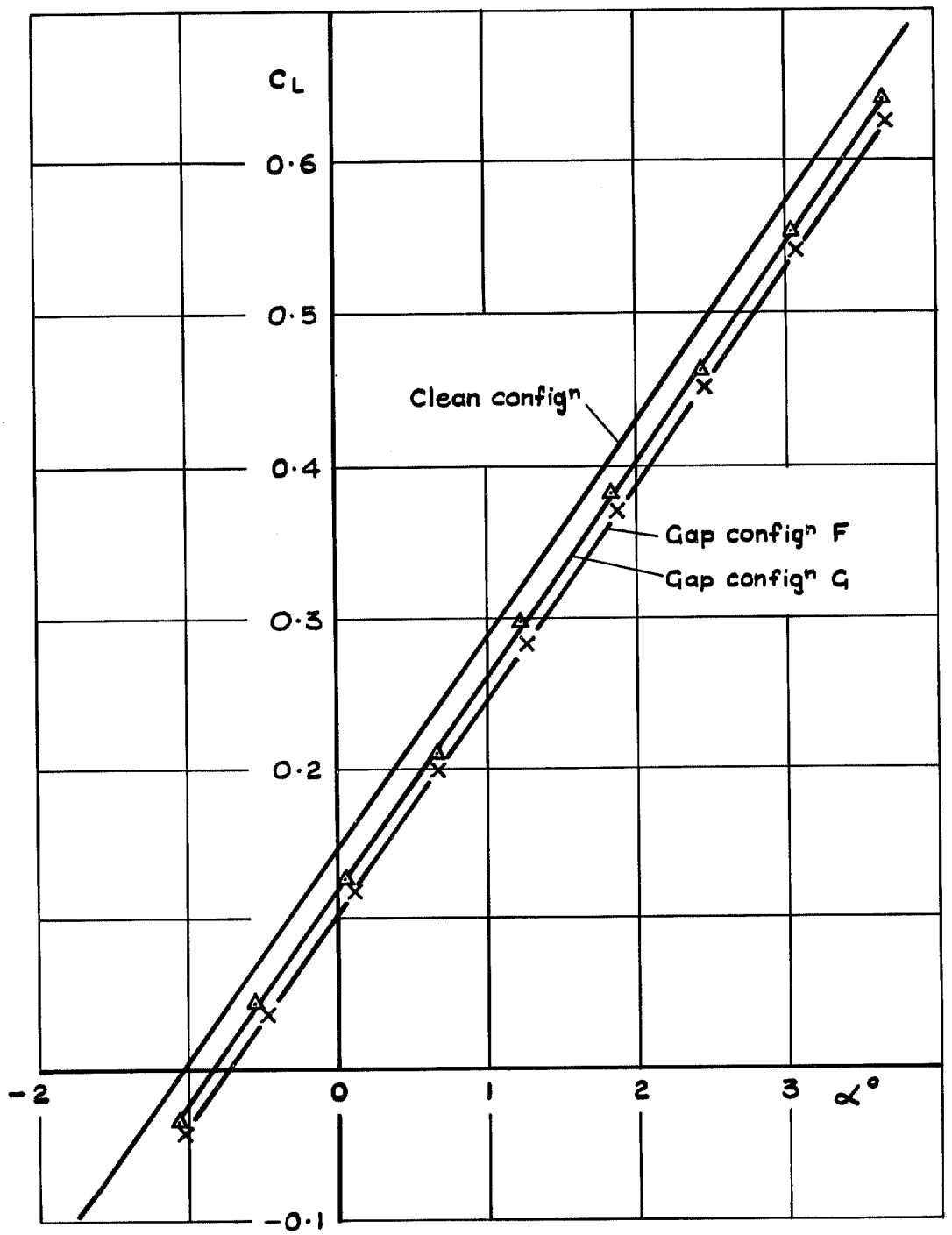

FIG. 17. Effect of chordwise gaps on C_L v α (configns F, G): $R = 15 \times 10^6$.

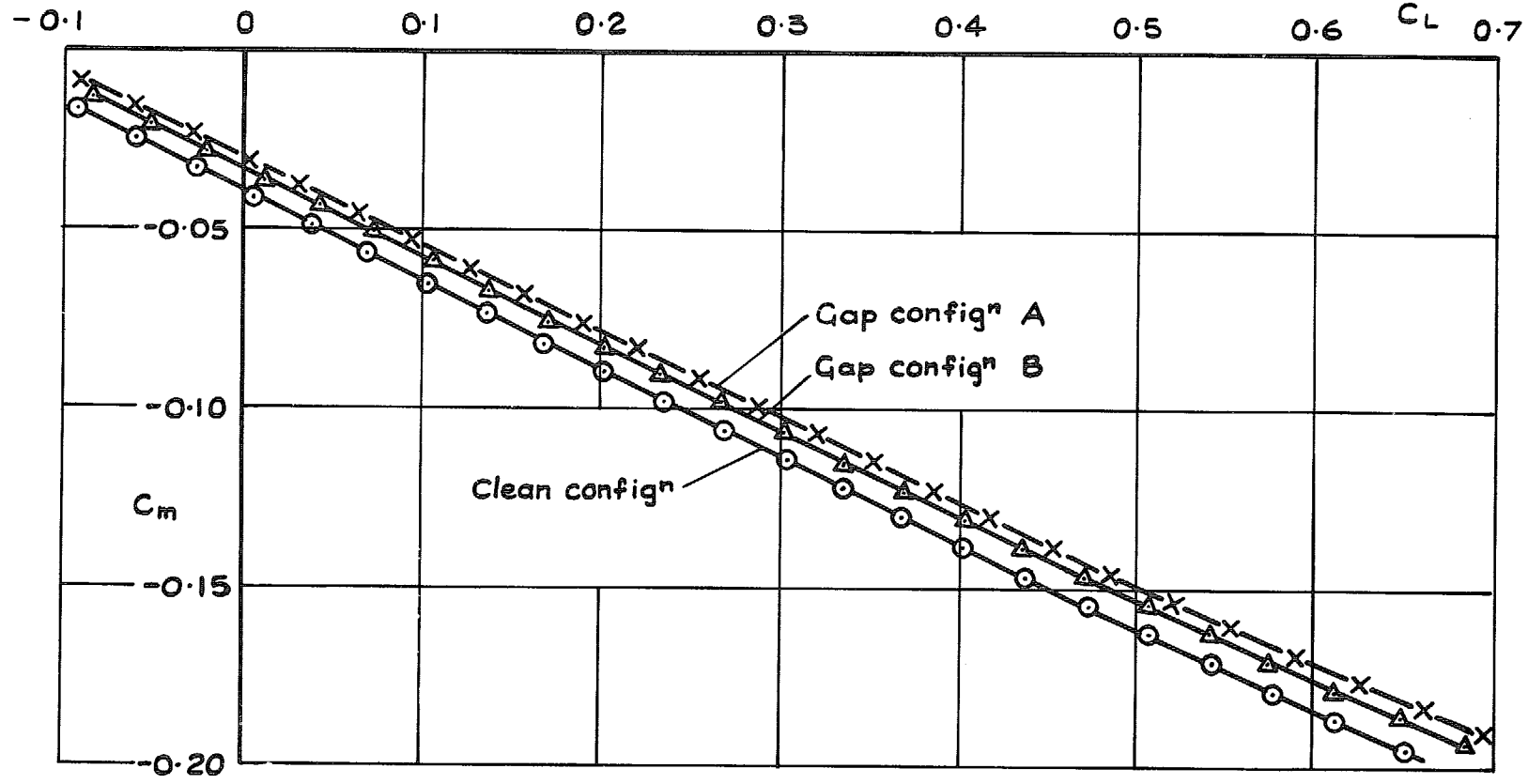

FIG. 18. Effect of spanwise gaps on C_m v C_L configns A and B: $R = 15 \times 10^6$.

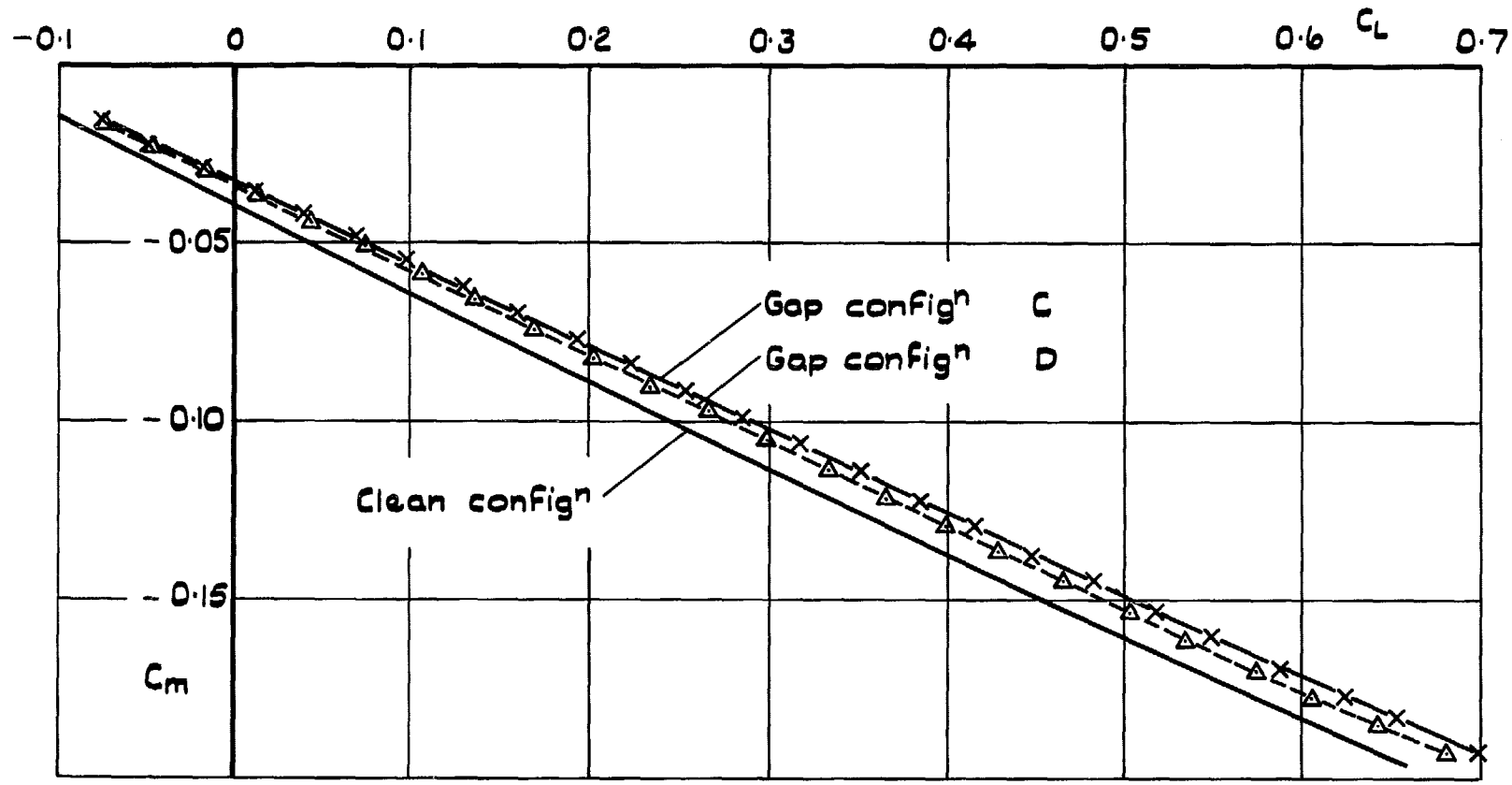

FIG. 19. Effect of spanwise gaps on C_m v C_L configns C and D: $R = 15 \times 10^6$.

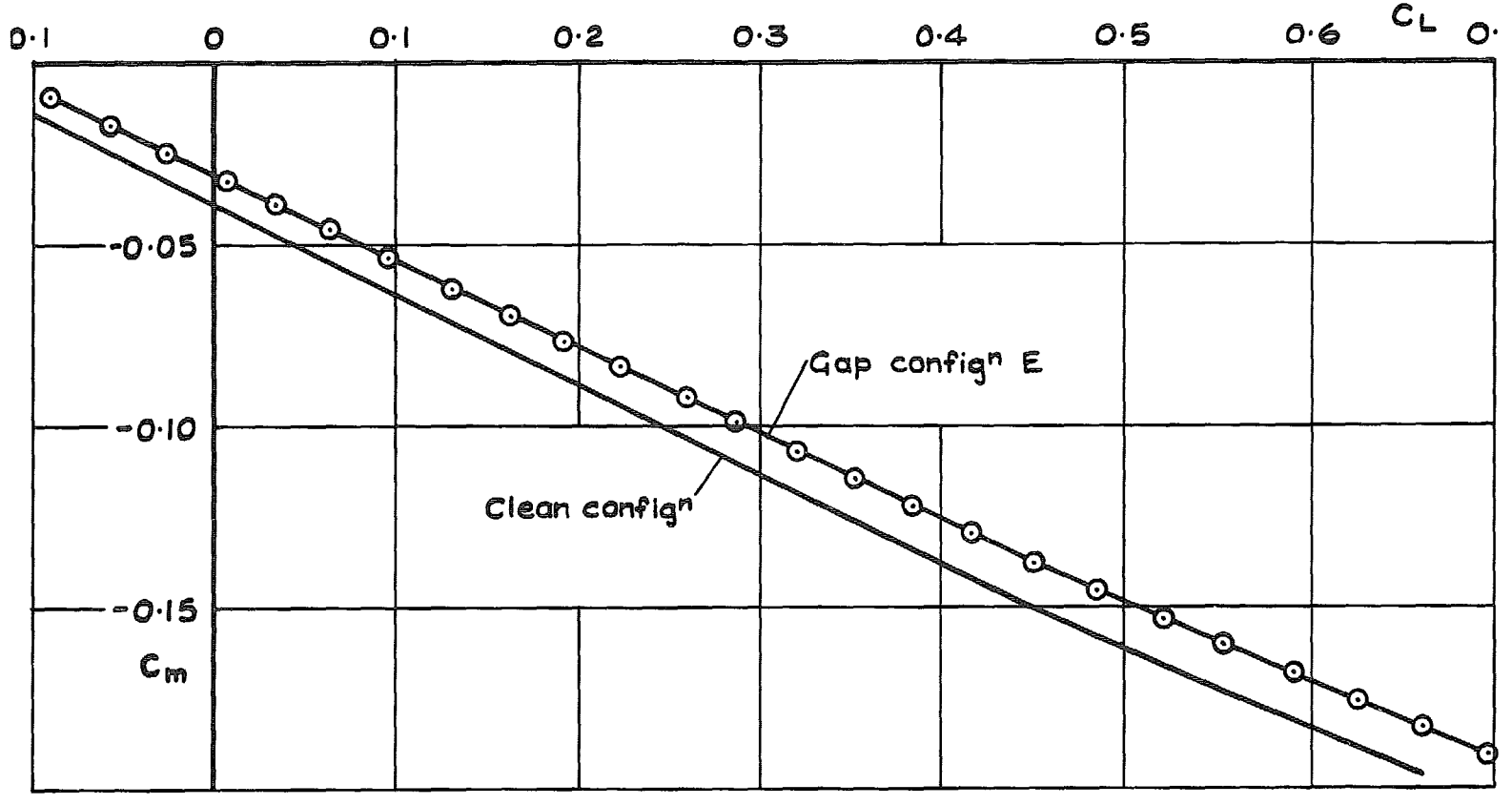

FIG. 20. Effect of spanwise gaps on C_m v C_L confign E: $R = 15 \times 10^6$.

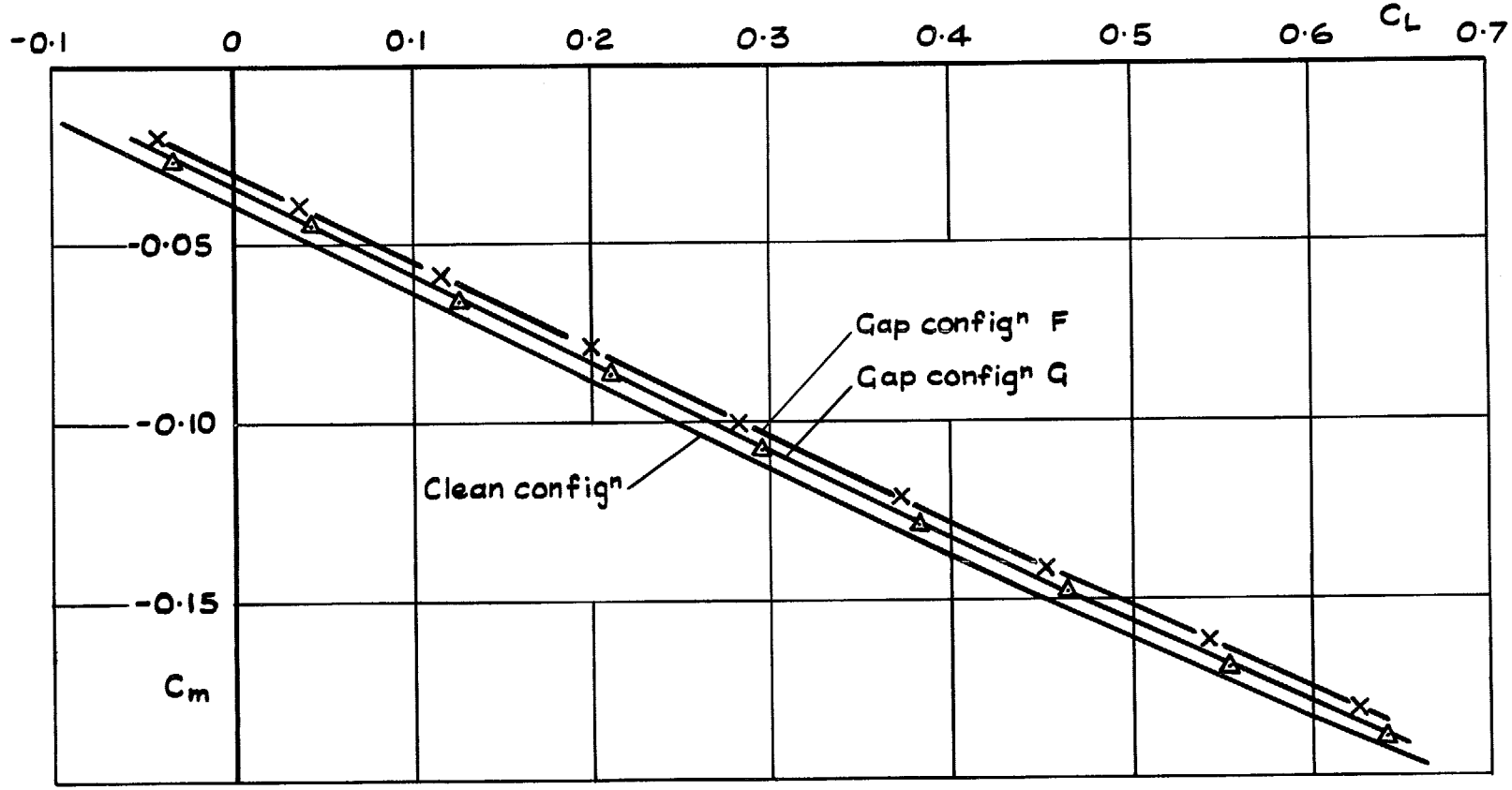

FIG. 21. Effect of chordwise gaps on C_m v C_L (gap configns F and G): $R = 15 \times 10^6$.

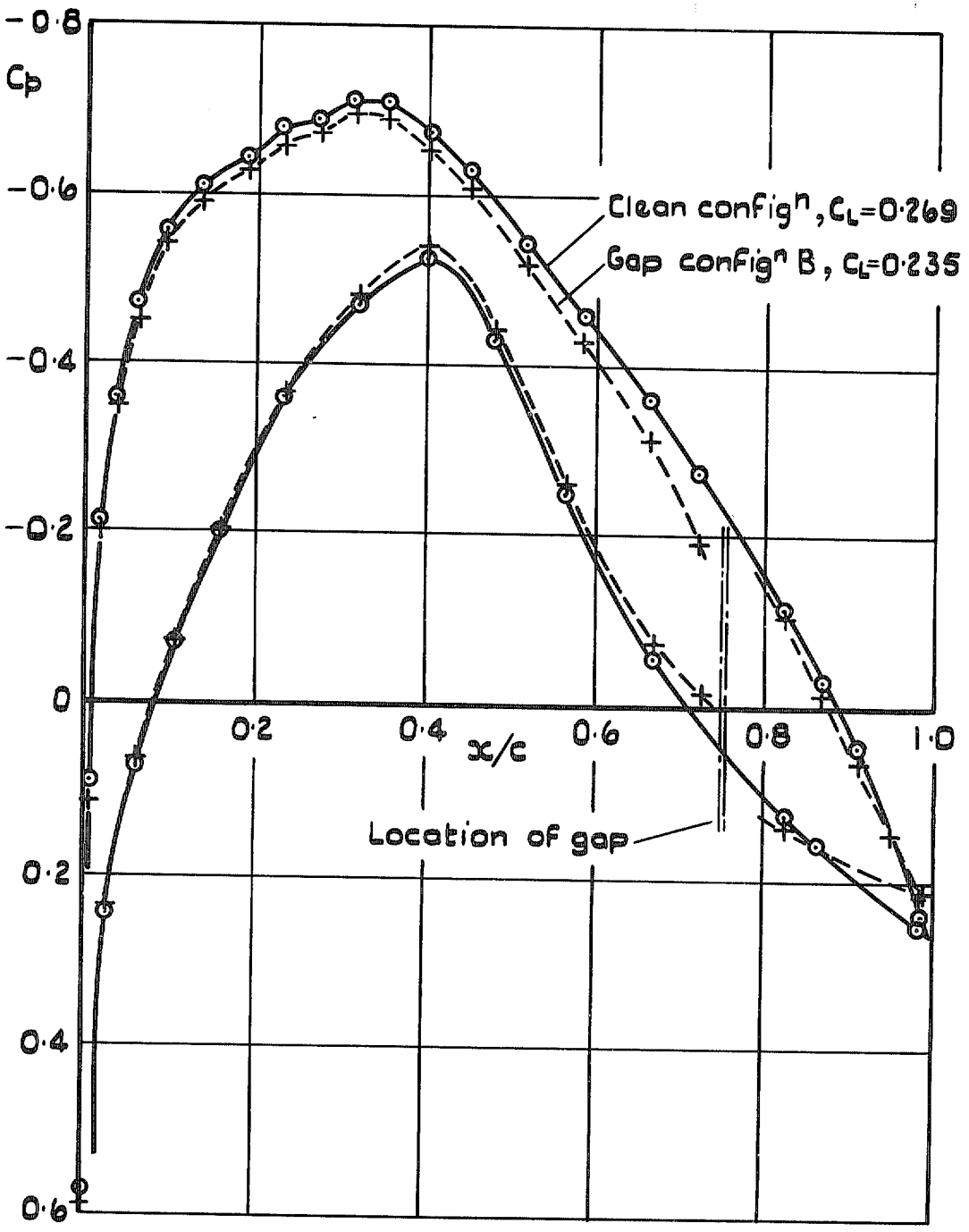

FIG. 22. Effect of spanwise gap on pressure distribution: config^n B; $R = 15 \times 10^6$, $\alpha = 0{\cdot}90°$.

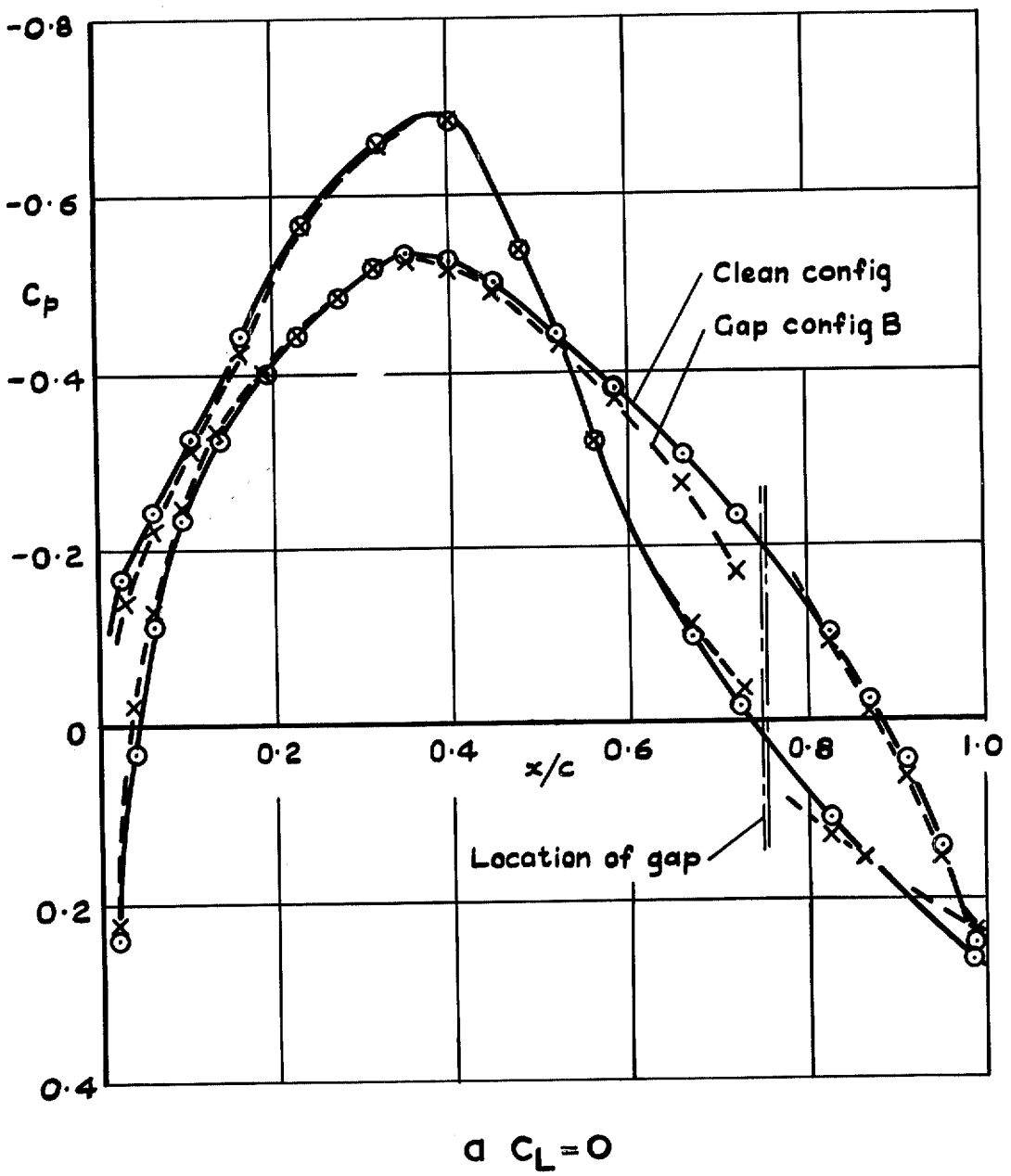

FIG. 23. Effect of spanwise gap on pressure distribution: confign B; $R = 15 \times 10^6$.

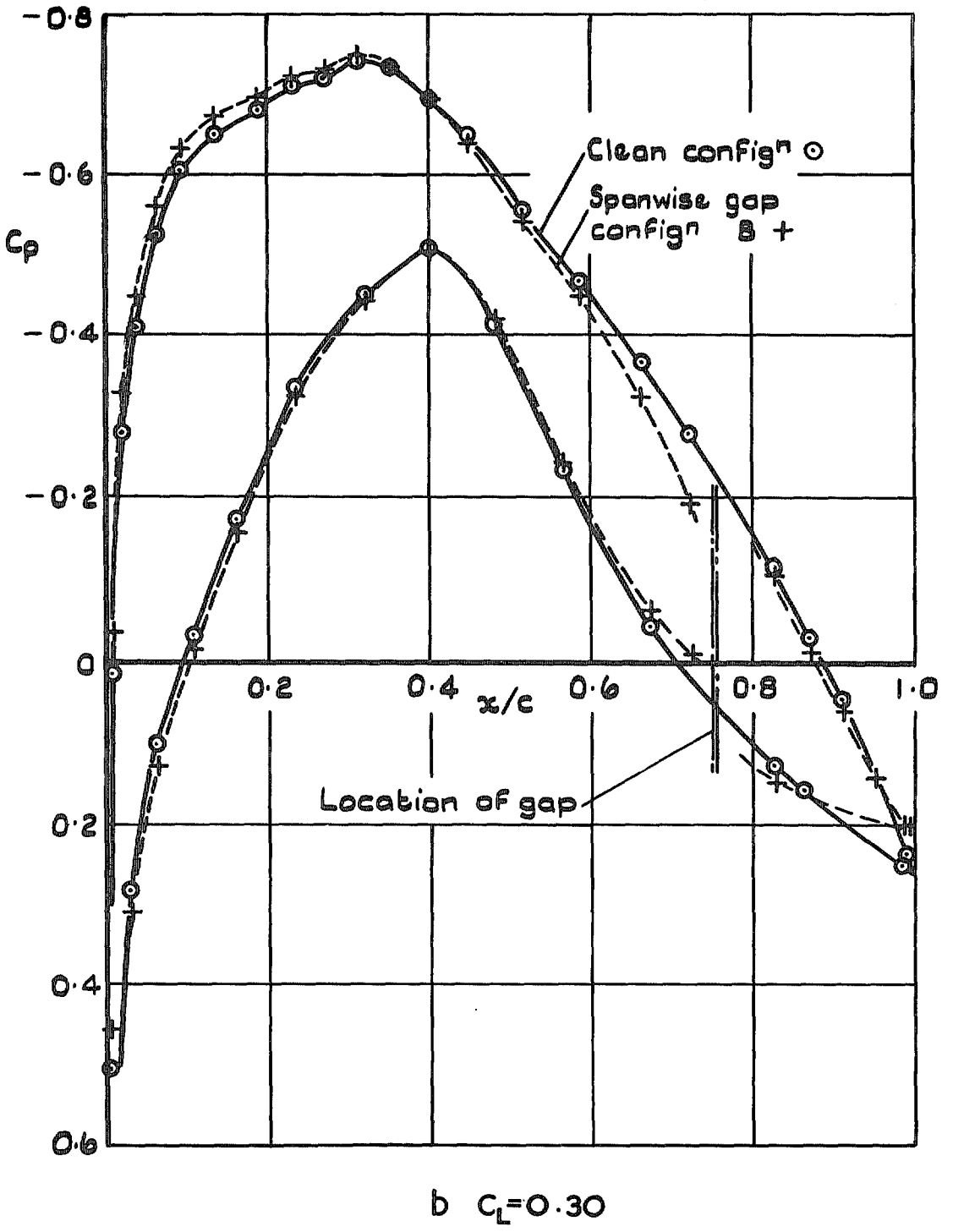

FIG. 23 contd. Effect of spanwise gap on pressure distribution: confign B: $R = 15 \times 10^6$.

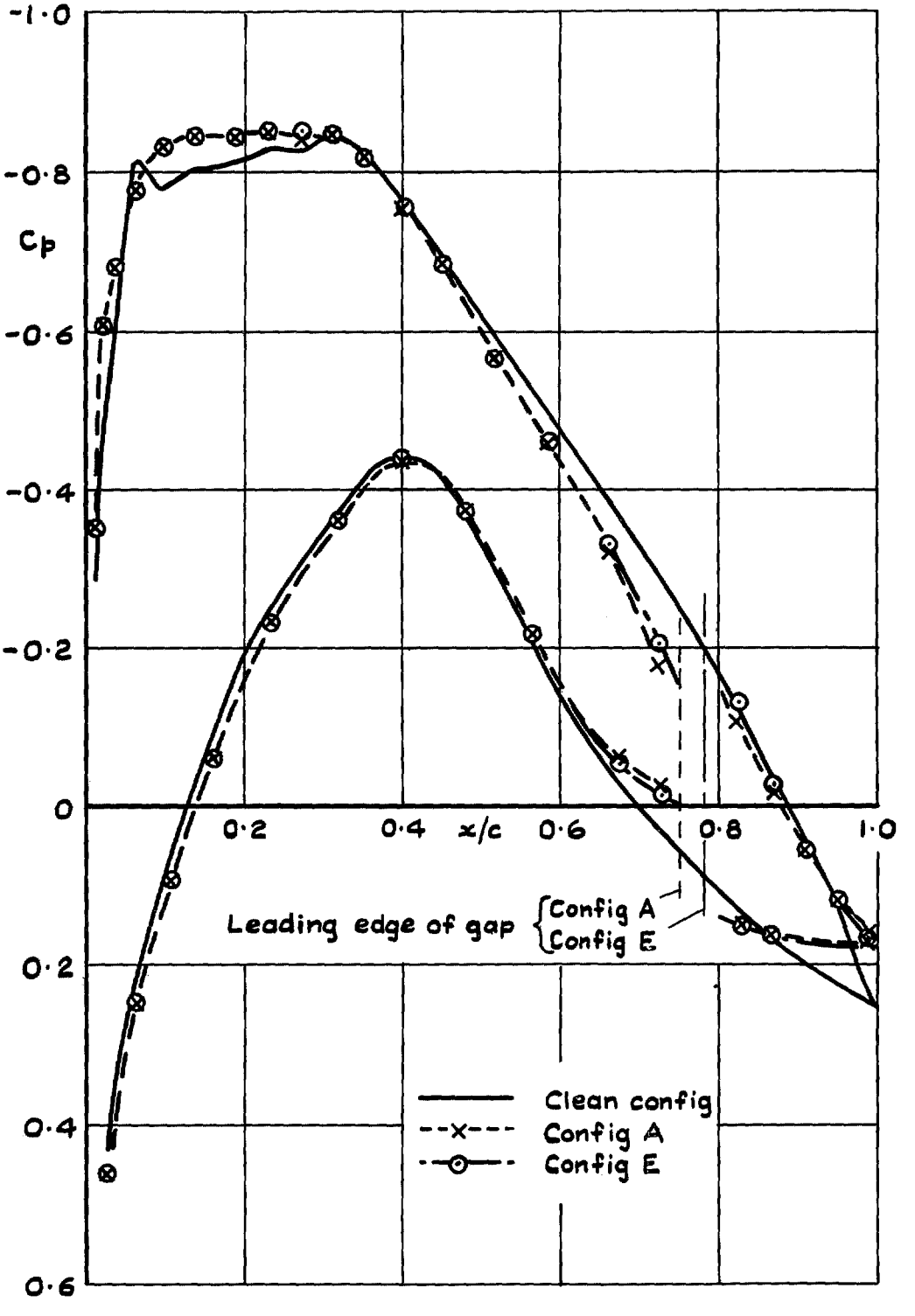

FIG. 24. Effect of spanwise gap on pressure distribution: configns A and E; $R = 15 \times 10^6$, $C_L = 0{\cdot}42$.

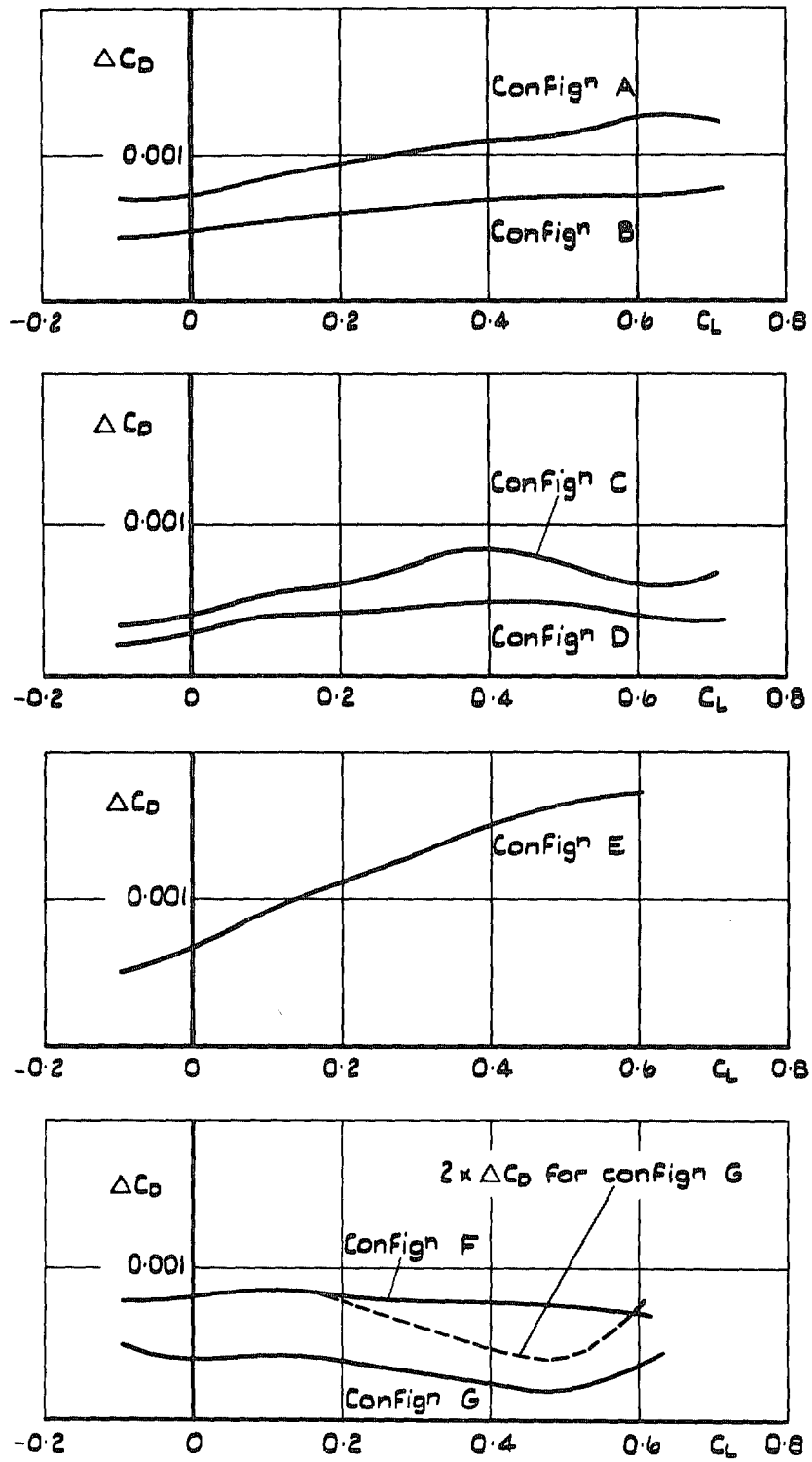

FIG. 25. Incremental drag due to gap: $R = 15 \times 10^6$.

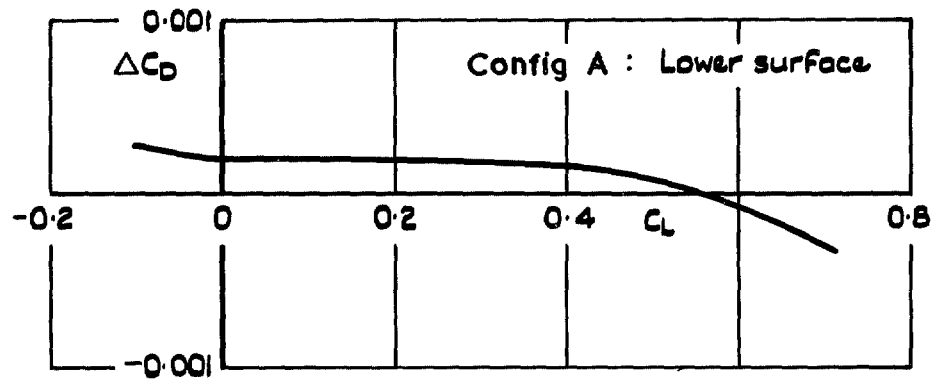

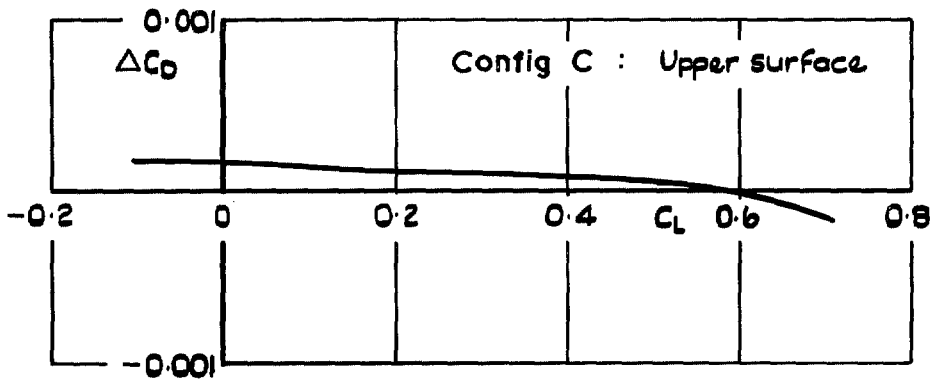

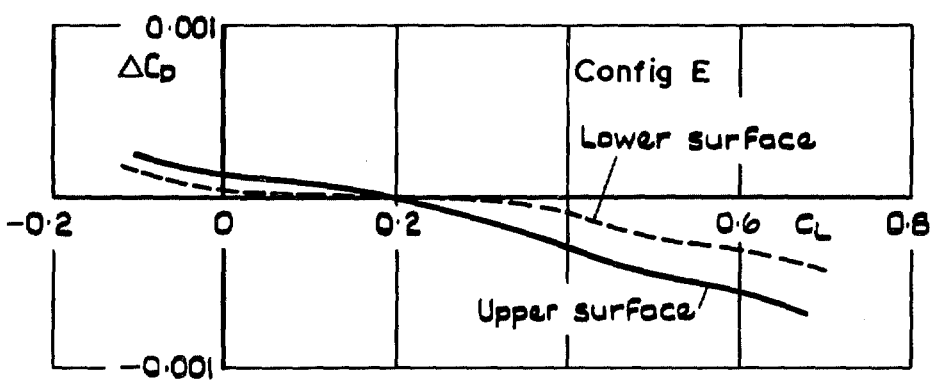

FIG. 26. Incremental drag due to slots: $R = 15 \times 10^6$.

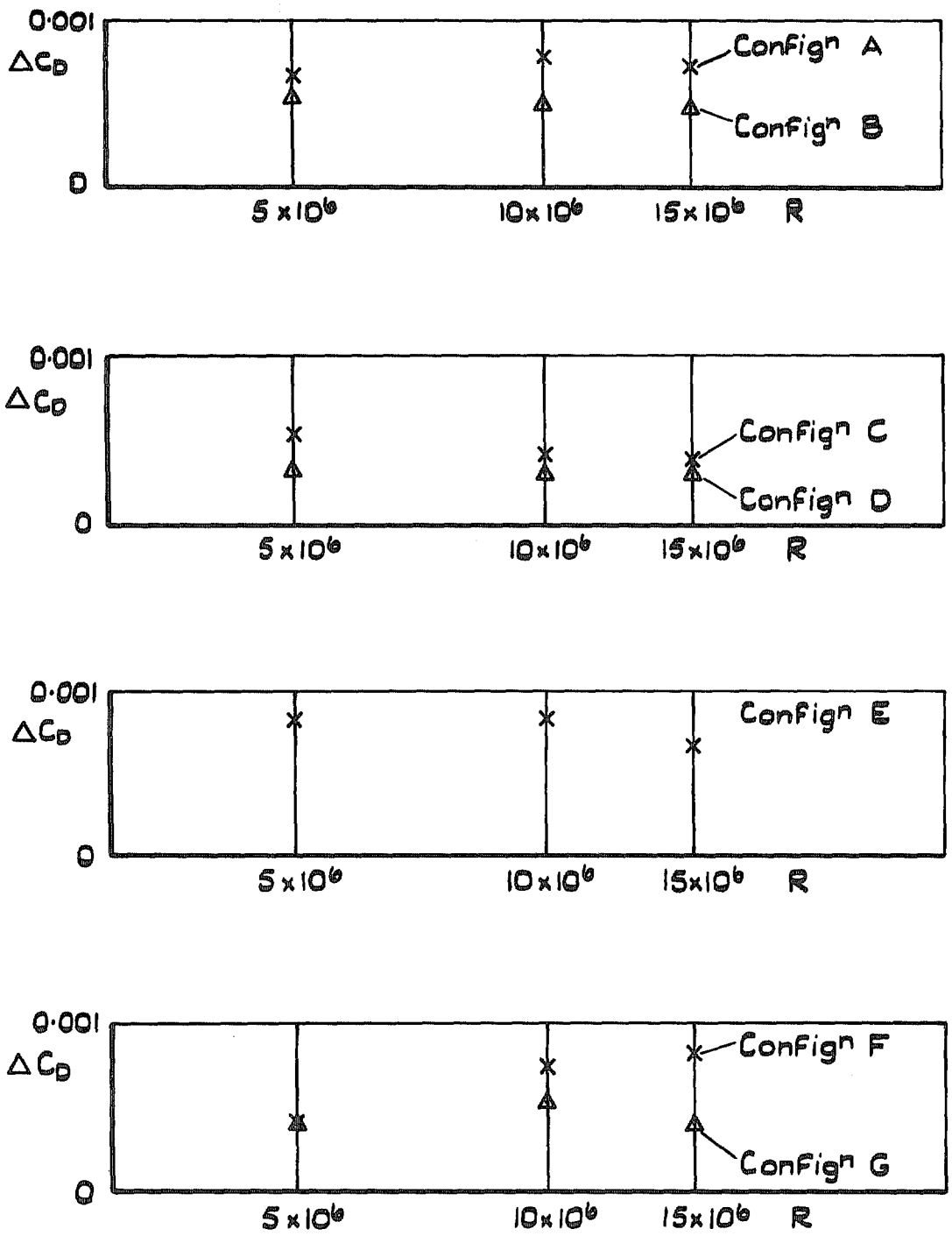

FIG. 27. Effect of Reynolds No. on drag due to gaps: zero lift.

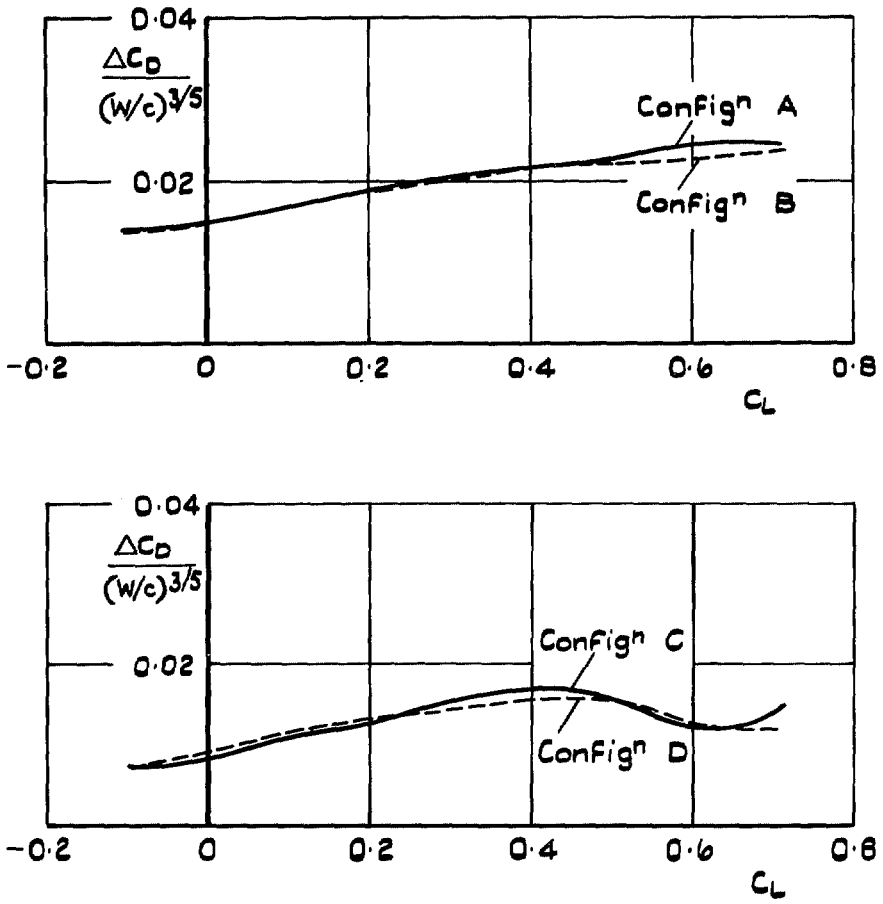

FIG. 28. Correlation of ΔC_D with spanwise gap width: $R = 15 \times 10^6$.

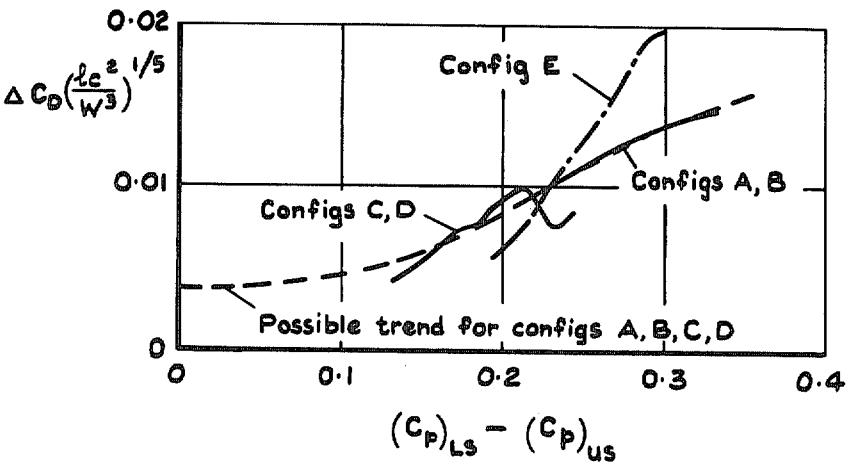

FIG. 29. Correlation of spanwise gap data: ($R = 15 \times 10^6$, $M = 0{\cdot}665$).

Printed in Wales for Her Majesty's Stationery Office by Allens Printers (Wales) Limited

Dd. 502110 K.5 6/72.

HER MAJESTY'S STATIONERY OFFICE

Government Bookshops

49 High Holborn, London WC1V 6HB
13a Castle Street, Edinburgh EH2 3AR
109 St Mary Street, Cardiff CF1 1JW
Brazennose Street, Manchester M60 8AS
50 Fairfax Street, Bristol BS1 3DE
258 Broad Street, Birmingham B1 2HE
80 Chichester Street, Belfast BT1 4JY

Government publications are also available through booksellers

SBN 11 470498 8